JOURNAL OF MAGNETIC RESONANCE **125,** 302–324 (1997)
ARTICLE NO. MN971110

One-Dimensional NOE Experiments Using Pulsed Field Gradients

KATHERINE STOTT,* JAMES KEELER,* QUE N. VAN,† AND A. J. SHAKA†

*Department of Chemistry, University of Cambridge, Lensfield Road, Cambridge CB2 1EW, United Kingdom; and
†Department of Chemistry, University of California, Irvine, California 92717

Received December 12, 1996

Previously, it has been shown that the use of pulsed field gradients in one-dimensional NOE experiments results in spectra of much higher quality than it has previously been possible to record. Such high-quality spectra make it possible to measure, with complete confidence, very small NOE enhancements and also make it straightforward to measure NOE buildup curves. In this paper, the spin dynamics behind these NOE experiments with gradients are analyzed in detail; the effects of strong coupling and molecular diffusion are also examined. It is also shown how the basic experiments can be improved upon, in particular how unwanted antiphase contributions (SPT effects) can be eliminated entirely. Experimental illustrations of the various methods and improvements are given and practical recommendations made as to how the experiments are best performed.

INTRODUCTION

The measurement of NOE enhancements by the steady-state NOE difference experiment is surely one of the most valuable experiments in the NMR arsenal (*1–4*). The experiment is uncomplicated, gives spectra which can be interpreted in a relatively straightforward way and, despite the limitation that the target resonances be well resolved, has wide applicability to small and medium-sized molecules. Two-dimensional NOESY (*5*) is the method of choice for measuring NOE enhancements in large molecules, such as proteins and nucleic acids, but has not been as attractive for smaller molecules where the NOE enhancements are weaker and as a complete set of enhancements is not usually needed.

The steady-state NOE difference experiment has some well-known problems, the most serious of which is the appearance in the difference spectrum of ''unwanted'' responses which arise from incomplete subtraction between the irradiated and control spectrum. The presence of these *subtraction artifacts* limits the reliability of the NOE difference spectra. Recently, we have made significant improvements to the quality of one-dimensional NOE spectra by introducing pulsed field gradients (PFGs) into the pulse sequences (*6, 7*); using these sequences, difference artifacts are eliminated. It is thus now possible to measure, with total confidence, NOE enhancements of as little as 0.02%, thus extending the range of distances over which the NOE can be used in a qualitative way. In addition, the improved quality of the data makes the measurement of NOE buildup curves much more straightforward, extending the use of the NOE as a quantitative tool.

In this paper, we investigate the detailed spin dynamics underlying these new one-dimensional NOE experiments and show how they differ from conventional experiments. We also show how interference effects associated with selective population transfer (SPT) and zero-quantum coherence can be eliminated. The effects of molecular diffusion and strong coupling are also considered. Finally, practical recommendations are made, and data illustrating the quality of both qualitative and quantitative measurements are shown.

The discussion in this paper is exclusively of one-dimensional NOE experiments. However, essentially the same principles apply to other selective experiments (*8*), such as those to measure rotating-frame NOE enhancements (*9*) or TOCSY-type experiments (*10*).

THEORY

Selective Excitation

Clean selective excitation of a single-spin multiplet is crucial to the success of any selective one-dimensional experiment, so it is not surprising that an enormous effort has been put into the design of selective-excitation methods, resulting in an almost bewildering array of possible choices. A recent addition to the range of selective-excitation methods is the idea of combining pairs of selective pulses with pulsed field gradients, a technique termed *excitation sculpting* (*7, 11, 12*). This technique offers flexible and high-quality selective excitation, and it will be used for all the experiments described in this paper. Full details of the excitation sculpting method are given elsewhere, and so we restrict ourselves here to a summary of the key points.

The heart of the excitation sculpting method is the double pulsed-field-gradient spin-echo (DPFGSE) sequence

1090-7807/97 $25.00

$$—[G_1—S—G_1—G_2—S—G_2]—, \quad [1]$$

where G_i represents a pulsed field gradient and S represents a radiofrequency pulse or sequence of pulses of any kind. If the gradients are sufficiently strong and chosen such that the first pair do not refocus the second, then it can be shown that, for a singlet, an initial magnetization vector, with components m_x, m_y, m_z along the x, y, and z axes respectively is transformed into a new vector with components M_x, M_y, M_z where

$$M_x = P^2 m_x,\ M_y = P^2 m_y,\ M_z = (1 - 2P)^2 m_z, \quad [2]$$

and where P is the probability that a spin is flipped by S; $0 \leqslant P \leqslant 1$. The DPFGSE sequence has the desirable property that it simply *scales* the amplitude of the magnetization and does not affect its phase; in addition, it does not mix different components of the magnetization.

The DPFGSE sequence can be used for selective excitation by choosing S to be a selective inversion pulse and then simply prefacing the whole sequence by a nonselective 90° pulse:

$$90°(\text{nonsel})—[G_1—S—G_1—G_2—S—G_2]—. \quad [3]$$

At offsets at which S is a perfect 180° pulse (e.g., on resonance), the spin is flipped so that $P = 1$ and according to Eq. [2] the DPFGSE sequence does not affect the magnetization. As the offset increases, the degree of inversion by S decreases, P falls, and the magnetization is attenuated. At sufficiently large offsets, S simply does not invert the spin at all, $P = 0$, and no magnetization survives the DPFGSE sequence. The excitation profile of the sequence of Eq. [3] thus mimics the inversion profile of the pulse S.

There are two key features of the excitation sequence of Eq. [3] which make it very suitable for use in one-dimensional NOE experiments. First, magnetization from spins with offsets outside the excitation bandwidth is dephased by the gradients. In a selective one-dimensional experiment, it is always necessary to suppress such magnetization, and it will be seen below that this is much easier to achieve in the case that the magnetization is dephased rather than, for example, being on the z axis.

The second key feature of excitation using the DPFGSE sequence is that the phase of the resulting magnetization does not vary with offset. In the following section, it is shown that as a consequence the amount of anti-phase magnetization which is generated when a multiplet is excited selectively is minimized and this in turn minimizes unwanted anti-phase contributions to the NOE spectra.

Excitation of Multiplets

The analysis of the result of selective excitation of a multiplet is straightforward if it can be assumed that the weak-coupling limit applies and that the selective pulses affect only the target spin, spin 1, and none of the coupled spins 2, 3. . . . If this is the case the lines of the spin 1 multiplet can simply be treated as separate resonances, each of which may in general be excited with a different phase and amplitude according to its offset.

The resulting magnetization from the multiplet as a whole can be analyzed into a sum of in-phase and anti-phase terms

$$\begin{aligned} &c_1^{(x)} I_{1x} + c_1^{(y)} I_{1y} + c_{12}^{(x)} 2I_{1x}I_{2z} + c_{12}^{(y)} 2I_{1y}I_{2z} \\ &\quad + c_{13}^{(x)} 2I_{1x}I_{3z} + c_{13}^{(y)} 2I_{1y}I_{3z} + \cdots \\ &\quad + c_{123}^{(x)} 4I_{1x}I_{2z}I_{3z} + c_{123}^{(y)} 4I_{1y}I_{2z}I_{3z} + \cdots, \end{aligned} \quad [4]$$

where the coefficients, $c_{i\ldots}^{(\alpha)}$, depend on the details of the excitation scheme and the couplings present. In an NOE experiment, the magnetization of the target spin must be rotated to the $-z$ axis, for example, by the application of a nonselective 90° pulse about $-x$ which rotates the term I_{1y} to $-I_{1z}$. Such a pulse will also affect the anti-phase terms, turning them into both single- and multiple-quantum coherences. Of these coherences, all but the zero-quantum contribution are easily removed by subsequent application of a field gradient pulse. It will be seen below that it is desirable to avoid generating zero-quantum coherences as they lead to unwanted anti-phase contributions in the final spectrum.

If a DPFGSE-based selective excitation scheme is used, such as that of Eq. [3], the magnetization produced has a constant phase (say, along the x axis). Half the terms (i.e., those containing the operator I_{1y}) of Eq. [4] are thus eliminated immediately, and along with them half the contributions to the unwanted zero-quantum coherence. If the amplitude of excitation is identical for all the lines of the multiplet, then the only operator generated is I_{1x}; the effect of uneven excitation is to generate terms such as $2I_{1x}I_{jz}$ and $2I_{1x}I_{jz}I_{kz}$. If, however, the excitation is symmetrical about the center of the multiplet, no singly anti-phase terms are generated as these inherently have a sign inversion when reflected about their center point. Doubly anti-phase terms have the required symmetry and so do contribute. The effect of different excitation profiles in terms of the product operators produced is illustrated in Fig. 1. It is clear that single phase and even excitation of the lines in the multiplet gives the optimum result.

Excitation with Phase Labeling

As described so far, the excitation scheme excites the magnetization of the target spin and dephases all other magnetization. An alternative is to set the gradients such that the magnetization from the target spin is phase encoded

$$90°(\text{nonsel})—[G_1—S—\bar{G}_1—\bar{G}_2—S—G_2]—, \quad [5]$$

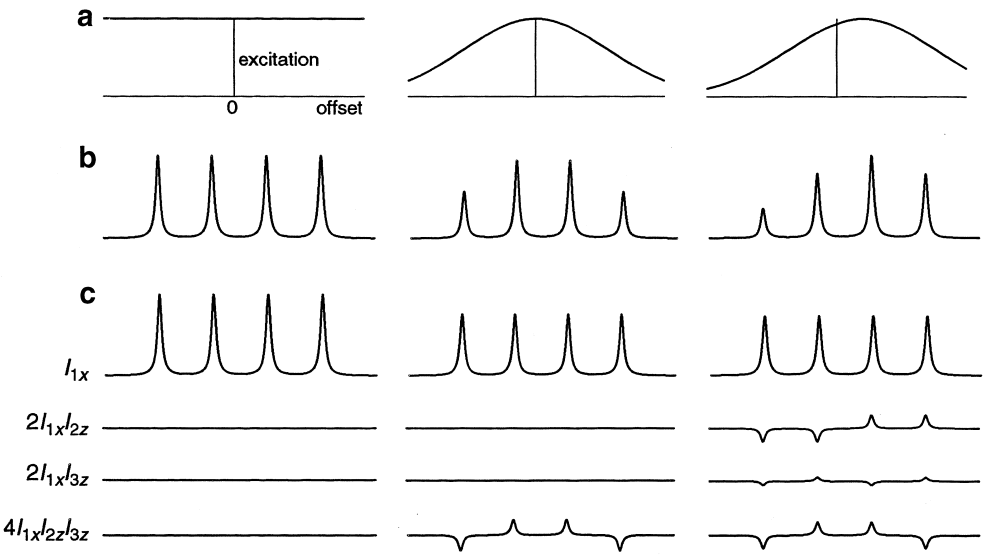

FIG. 1. Illustration of the way in which uneven excitation of the lines of a multiplet lead to the generation of anti-phase terms; a doublet of doublets associated with spin 1 and with $J_{12} > J_{13}$ is used as an example. Three different excitation profiles are shown in (a): on the left a perfect profile with even amplitude at all offsets, in the middle a symmetric profile, and on the right an asymmetric profile. The form of the multiplet which would be excited by each profile is shown in (b). Shown in (c) is the analysis of each multiplet into contributions from in-phase, singly anti-phase, and doubly anti-phase operators. The perfect profile leads to the generation of only in-phase magnetization, I_{1x}; the symmetric profile also leads to the generation of some doubly anti-phase magnetization, $4I_{1x}I_{2z}I_{3z}$; and the asymmetric profile in addition leads to the generation of singly anti-phase terms, $2I_{1x}I_{2z}$ and $2I_{1x}I_{3z}$.

where the overbar indicates a gradient applied in the opposite sense. In this sequence, magnetization is dephased by G_1 and, if it experiences S as a refocusing pulse, continues to be dephased by $\bar{G}_1$ and $\bar{G}_2$ and then, after a second refocusing pulse, by G_2. The final result is that the magnetization from the target spin is excited and acquires a phase label according to the length and strength of all four gradients; a subsequent refocusing gradient will be needed in order to make this magnetization observable. Magnetization from all other spins which do not experience S as a refocusing pulse is dephased by G_1 but then rephased by $\bar{G}_1$; likewise G_2 refocuses the dephasing caused by $\bar{G}_2$. The final result is that this magnetization has no phase label and is thus distinguishable from magnetization of the target spin. In all other respects, the sequence has the same properties as the sequence shown in Eq. [3].

In practice, it will be the case that the pulse S has some effect, albeit rather small, on the coupled spins, and so the simple analysis in which a multiplet is treated as a series of independent lines is not strictly valid. In addition, although at the end of the DPFGSE sequence spins other than the target are not excited to a significant extent, it may nevertheless be the case that *during* S the spins are excited. An analysis which takes into account such effects is considerably more complex than the single-transition approach which is commonly used to assess selective-excitation methods. Broadly speaking, the result of taking into account the presence of other spins is the appearance of anti-phase terms with greater intensity than expected on the basis of a simple analysis. The details of which terms appear and their magnitudes depends in a complex way on the nature of S, the length of the gradients, and the parameters of the spin system.

GOESY

The GOESY experiment was the first one-dimensional NOE experiment which employed pulsed field gradients as part of the selective-excitation process (*6*). A variant of the original sequence is shown in Fig. 2a. The first part is simply a DPFGSE selective-excitation sequence of the type described above, Eq. [5], which generates phase-labeled magnetization of the target spin. A nonselective 90° pulse rotates part of this magnetization to the z axis, creating a nonequilibrium state; during the mixing time, τ_m, magnetization is transferred between spins which cross-relax one another. A gradient, G_m, applied during the mixing time eliminates all but z magnetization and zero-quantum coherence. At the end of the mixing time, a further nonselective 90° read pulse generates transverse magnetization, and a final gradient, G_3, refocuses the phase label accrued during the DPFGSE sequence. Chemical-shift (offset) evolution during the final gradient is refocused by placing it in a nonselective spin echo.

The final result is that the only magnetization which is refocused, and hence observed, is that of the target spin, or magnetization arising from cross relaxation with the target spin. The spectrum shows just the target resonance and any resonances from spins which cross-relax with the target spin.

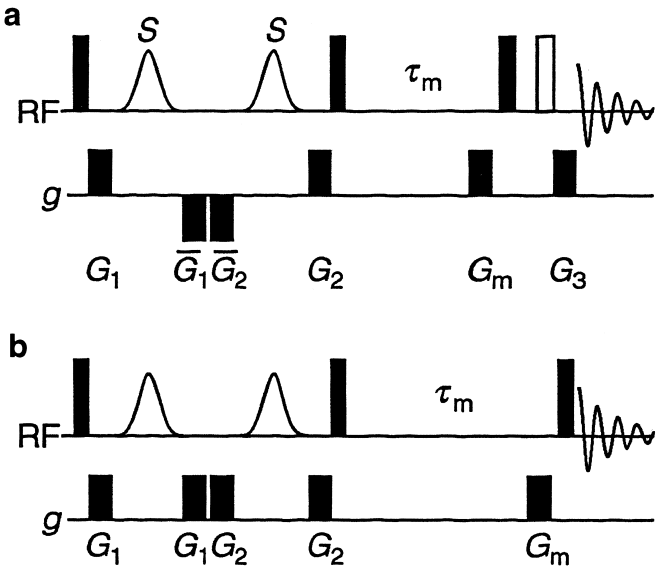

FIG. 2. Basic pulse sequences for recording one-dimensional NOE spectra. Radiofrequency pulses are indicated on the line marked RF: the solid and open rectangles are nonselective 90° and 180° pulses, respectively, and selective shaped pulses are indicated by their envelopes. All pulses have phase *x* unless otherwise stated. Gradient pulses are indicated on the line marked *g*. Sequence (a) is for the GOESY experiment with DPFGSE excitation; sequence (b) is for the DPFGSE NOE experiment.

An NOE spectrum is thus recorded *in a single scan*, without resort to any difference methods, and as a result, the spectra are extraordinarily clean and free from subtraction artifacts.

The GOESY sequence can be analyzed using the Solomon equations for two spins, which will be written

$$\frac{dM_{1z}}{dt} = -R_1(M_{1z} - M_0) - \sigma_{12}(M_{2z} - M_0)$$

$$\frac{dM_{2z}}{dt} = -\sigma_{12}(M_{1z} - M_0) - R_2(M_{2z} - M_0), \qquad [6]$$

where M_0 is the equilibrium z magnetization on spin 1 or 2 (assumed to be have the same value), R_i is the self-relaxation rate constant of spin i, and σ_{ij} is the cross-relaxation rate constant between spins i and j. Taking the pulse phases as in Fig. 2a, at the end of the excitation sequence (after G_2), the state of the target spin, spin 1, may be written

$$\alpha_1[-\cos\,\phi(r)I_{1y} + \sin\,\phi(r)I_{1x}], \qquad [7]$$

where $\phi(r)$ is the spatially dependent phase which results from the four gradients in the DPFGSE sequence and α_1 is a parameter representing the degree of excitation of spin 1. If the selective excitation is perfect, $\alpha_1 = 1$, but if magnetization is lost due to the generation of anti-phase states or relaxation, $\alpha_1 < 1$. The 90° pulse at the start of the mixing time rotates the y component of the magnetization onto the z axis; the remaining transverse component is not involved in cross relaxation and will be dephased by G_m. Thus, at the start of the mixing time, the relevant magnetization of the target spin is

$$-\alpha_1\cos\,\phi(r)I_{1z}. \qquad [8]$$

For the other spin, spin 2, we shall assume that the DPFGSE sequence has no effect and, at the start of the mixing time, write the state of this spin as

$$\alpha_2 I_{2z}, \qquad [9]$$

where the parameter α_2, $-1 \leqslant \alpha_2 \leqslant 1$, accounts for two effects. First, during the DPFGSE sequence, the transverse magnetization of spin 2 will precess according to its offset and as a consequence the amount of z magnetization created by the 90° pulse at the start of the mixing time will depend on the offset. Second, there may be losses due to relaxation or pulse imperfections which will reduce the size of the z magnetization generated.

The situation at the start of the mixing time is somewhat unusual for an NOE experiment, as the state of spin 1 depends, via Eq. [8], on the spatially dependent phase. Thus as we move through the sample, there is a continuous variation of starting points from which an NOE enhancement may build up. Assuming for simplicity that both α_1 and α_2 are unity, it can be seen that if $\phi(r) = 0$ spin 1 is inverted and spin 2 is at equilibrium whereas at another position at which $\phi(r) = \pi$, both spins are at equilibrium. All situations between these two extremes are also present. The detailed dynamics of the cross-relaxation process is thus different at different points in the sample.

It is instructive to make an analysis in the initial rate regime. Starting with the initial conditions of Eqs. [8] and [9], the Solomon equations become

$$\left(\frac{dM_{1z}}{dt}\right)_{\text{initial}} = R_1[1 + \alpha_1\cos\,\phi(r)]M_0 + \sigma_{12}(1 - \alpha_2)M_0$$

$$\left(\frac{dM_{2z}}{dt}\right)_{\text{initial}} = \sigma_{12}[1 + \alpha_1\cos\,\phi(r)]M_0 + R_2(1 - \alpha_2)M_0, \qquad [10]$$

where, for simplicity, we have assumed that $\langle I_{iz}\rangle = M_0$. Solving these in this initial rate limit gives

$$\frac{M_{1z}(\tau_m)}{M_0} = \{R_1[1 + \alpha_1 \cos\phi(r)] + \sigma_{12}(1 - \alpha_2)\}\tau_m - \alpha_1 \cos\phi(r)$$

$$\frac{M_{2z}(\tau_m)}{M_0} = \{\sigma_{12}[1 + \alpha_1 \cos\phi(r)] + R_2(1 - \alpha_2)\}\tau_m + \alpha_2. \quad [11]$$

The nonselective 90° pulse (assumed for convenience to be about the *y* axis) at the end of the mixing time makes these longitudinal terms transverse and the final gradient, G_3, refocuses the dephasing caused by the excitation sequence. Only the terms which have a spatially dependent phase will be refocused by the final gradient, other terms will be dephased and hence lost. Retaining, therefore, just the terms dependent on $\phi(r)$, the transverse magnetizations of spin 1 and spin 2 present prior to the final gradient are

$$\frac{M_{1x}(\tau_m)}{M_0} = \alpha_1 \cos\phi(r)[R_1\tau_m - 1]$$

$$\frac{M_{2x}(\tau_m)}{M_0} = \alpha_1\sigma_{12}\tau_m \cos\phi(r), \quad [12]$$

where τ_m is the mixing time. The effect of the final gradient is simply to add an additional phase to these terms, representing their evolution in the *xy* plane

$$\frac{M_1(\tau_m)}{M_0} = \alpha_1 \cos\phi(r)[R_1\tau_m - 1]\exp[i\phi'(r)]$$

$$\frac{M_2(\tau_m)}{M_0} = \alpha_1\sigma_{12}\tau_m \cos\phi(r)\exp[i\phi'(r)], \quad [13]$$

where $\phi'(r)$ is the spatially dependent phase induced by the final gradient, G_3, and M_i is transverse magnetization of spin *i* after the final gradient and represented as a complex number: $M_i = M_x + iM_y$. By expanding the cosine in terms of exponentials we obtain

$$\frac{M_1(\tau_m)}{M_0} = \alpha_1 \frac{1}{2}\{\exp[i\phi(r)] + \exp[-i\phi(r)]\} \times [R_1\tau_m - 1]\exp[i\phi'(r)]$$

$$\frac{M_2(\tau_m)}{M_0} = \alpha_1\sigma_{12}\tau_m \frac{1}{2}\{\exp[i\phi(r)] + \exp[-i\phi(r)]\} \times \exp[i\phi'(r)] \quad [14]$$

from which it is clear that by choosing $\phi'(r) = +\phi(r)$ or $-\phi(r)$ one-half of the signal can be refocused. The loss of half the signal when gradients are used for coherence selection is a familiar phenomenon; it arises because the final gradient can be set to refocus coherence which starts out after the first pulse as either coherence order -1 or $+1$, but not both. The refocused observable signals are thus

$$\frac{M_1(\tau_m)}{M_0} = \frac{1}{2}\alpha_1(R_1\tau_m - 1)$$

$$\frac{M_2(\tau_m)}{M_0} = \frac{1}{2}\alpha_1\sigma_{12}\tau_m. \quad [15]$$

From these expressions, it can be seen that the only spin-2 magnetization present is due to cross relaxation. There is no need for difference spectroscopy—the GOESY spectrum shows just the NOE-enhanced resonances and the lines from the target spin. In this experiment, the ratio $[M_i(\tau_m)/M_0]$ can be identified as the NOE enhancement factor, η_i, of spin *i*; in the initial rate limit, the enhancement builds up with a rate constant of $\frac{1}{2}\alpha_1\sigma_{12}$. The signal from spin 1, the target, will be close to its starting value and, in the positive NOE region, opposite in sign to that of spin 2.

It is useful at this point to compare the outcome of the GOESY experiment with the conventional transient NOE experiment which can be represented

180°(selective to spin 1; on/off)—τ_m—90°(nonsel)—acquire (+/−).

This is a difference method in which two experiments are performed: the first, which leads to what we term the *irradiated spectrum*, has the selective 180° pulse on resonance and the second, which leads to the *reference spectrum*, has the pulse off resonance. The difference between these two, which can be calculated in the time or frequency domain, gives the NOE difference spectrum.

For the case where the 180° pulse is on-resonance, the starting position for the magnetization on spin 1 is $-\alpha_1 I_{1z}$ and spin 2 is at equilibrium. In the initial rate limit, the magnetizations at the end of the mixing time are

$$\frac{M_{1z}(\tau_m)}{M_0} = [R_1(1 + \alpha_1)]\tau_m - \alpha_1$$

$$\frac{M_{2z}(\tau_m)}{M_0} = [\sigma_{12}(1 + \alpha_1)]\tau_m + 1. \quad [16]$$

When recording the reference spectrum, the 180° pulse is off-resonance and has no effect; the resulting magnetization, $M_{iz,ref}$, is simply M_0. The magnetization which contributes to the difference spectrum can thus can calculated as

$$\frac{M_{1z}(\tau_m) - M_{1z,ref}}{M_0} = \frac{M_{1z}(\tau_m) - M_0}{M_0}$$
$$= [R_1(1 + \alpha_1)]\tau_m - \alpha_1 - 1$$
$$\frac{M_{2z}(\tau_m) - M_{2z,ref}}{M_0} = \frac{M_{2z}(\tau_m) - M_0}{M_0}$$
$$= [\sigma_{12}(1 + \alpha_1)]\tau_m. \quad [17]$$

For a difference experiment, the NOE enhancement, η_i, is defined as $[(M_{iz}(\tau_m) - M_0)/M_0]$, so from Eq. [17] it is seen that spin 2 will receive an NOE enhancement of size $\sigma_{12}(1 + \alpha_1)\tau_m$, and the rate constant for the initial buildup of the enhancement is $\sigma_{12}(1 + \alpha_1)$.

Assuming for the moment that the excitation or inversion of the target spin is perfect, i.e., $\alpha_1 = 1$, the buildup rate in GOESY is $\frac{1}{2}\sigma_{12}$, whereas in the transient NOE experiment the rate is $2\sigma_{12}$, i.e., the buildup rate in GOESY is one-quarter of that in the transient NOE experiment. This reduction can be understood in the following way: a factor of one-half comes about due to the fact that only half the magnetization can be recovered by the final gradient; a second factor of one-half comes about because, when averaged over the sample, in a GOESY experiment the magnetization of the target spin starts out as being saturated rather than inverted as is the case in the conventional experiment.

This last point is worth some further comment. The starting magnetization on the target spin in the GOESY experiment is $-\cos\phi(r)M_0$ so that the cross-relaxation term in the Solomon equation for spin 2, Eq. [6], is

$$\sigma_{12}(M_z - M_0) = \sigma_{12}(\cos\phi(r) + 1)M_0. \quad [18]$$

Along the sample, $\cos\phi(r)$ varies between -1 and $+1$, so the cross-relaxation term varies between $2\sigma_{12}M_0$ and zero. Averaged over the sample, therefore, the cross-relaxation term is $\sigma_{12}M_0$ which is precisely the starting point for an experiment in which the target spin is saturated. In this respect, GOESY is thus analogous to a *transient* NOE experiment in which the target spin is *saturated*.

In comparing the sensitivity of GOESY with a conventional transient NOE experiment, we also need to take account that in the transient experiment one-half of the experiment time is used for recording the reference spectrum which is subsequently subtracted from the irradiated spectrum. It follows that in a fixed experiment time the signal-to-noise ratio of the transient experiment is *twice* that of GOESY. It will be seen later that molecular diffusion further reduces the sensitivity of GOESY.

The Solomon equations can be solved explicitly for each experiment to give the following time dependence of the NOE enhancements, η,

$$\eta_{GOESY} = \frac{M_{2z}(\tau_m)}{M_0}$$
$$= \frac{\alpha_1\sigma_{12}}{2\rho}\left\{\exp\left[-(R_1 + R_2 - \rho)\frac{\tau_m}{2}\right] - \exp\left[-(R_1 + R_2 + \rho)\frac{\tau_m}{2}\right]\right\} \quad [19]$$

$$\eta_{transient} = \frac{M_{2z}(\tau_m) - M_0}{M_0}$$
$$= \frac{(1 + \alpha_1)\sigma_{12}}{\rho}\left\{\exp\left[-(R_1 + R_2 - \rho)\frac{\tau_m}{2}\right] - \exp\left[-(R_1 + R_2 + \rho)\frac{\tau_m}{2}\right]\right\}, \quad [20]$$

where $\rho^2 = (R_1 - R_2)^2 + 4\sigma_{12}^2$. These time dependences are, apart from a simple scaling of the amplitudes, identical; at all times the ratio of the enhancements is

$$\frac{\eta_{GOESY}}{\eta_{transient}} = \frac{\alpha_1}{2(1 + \alpha_1)}. \quad [21]$$

In addition, the value of the parameter α_2 has no effect on the enhancement.

The maximum enhancement occurs, in both experiments, for a mixing time given by

$$\tau_{m,max} = \frac{1}{\rho}\ln\left(\frac{R_1 + R_2 + \rho}{R_1 + R_2 - \rho}\right), \quad [22]$$

and the maximum enhancements are

$$\eta_{GOESY,max} = \left(\frac{\alpha_1\sigma_{12}}{R_1 + R_2 - \rho}\right) \times \left(\frac{R_1 + R_2 + \rho}{R_1 + R_2 - \rho}\right)^{-[1+(R_1+R_2)/\rho]/2} \quad [23]$$

$$\eta_{transient,max} = \left(\frac{2(1 + \alpha_1)\sigma_{12}}{R_1 + R_2 - \rho}\right) \times \left(\frac{R_1 + R_2 + \rho}{R_1 + R_2 - \rho}\right)^{-[1+(R_1+R_2)/\rho]/2}. \quad [24]$$

For comparison, the maximum enhancement in a steady-state NOE experiment is

$$\eta_{SS,max} = \left(\frac{\sigma_{12}}{R_2}\right). \quad [25]$$

DPFGSE NOE

The DPFGSE NOE experiment (*7*), whose sequence is shown in Fig. 2b, differs from the GOESY experiment in that the gradients in the DPFGSE sequence are set so that the magnetization of the target spin is rephased and that of all other spins is dephased. The second nonselective 90° pulse therefore inverts that magnetization of the target spin, and so at the start of the mixing time the z magnetization for each spin is

$$M_{1z} = -\alpha_1 M_0 \quad \text{and} \quad M_{2z} = 0, \quad [26]$$

where, as before, the parameter α_1 is included to account for imperfections in the selective-excitation sequence. From the point of view of the target spin, the experiment is identical to the conventional transient NOE experiment; however, there is a difference in that in the DPFGSE NOE experiment all the other spins are saturated, rather than being at equilibrium. We shall see that this is key in the practical success of the DPFGSE NOE experiment.

Applying the initial rate approximation gives the following situation at the end of the mixing time

$$\frac{M_{1z}(\tau_m)}{M_0} = [(1 + \alpha_1)R_1 + \sigma_{12}]\tau_m - \alpha_1$$

$$\frac{M_{2z}(\tau_m)}{M_0} = [R_2 + (1 + \alpha_1)\sigma_{12}]\tau_m. \quad [27]$$

In contrast to the case for GOESY (Eq. [12]), there are two terms contributing to the magnetization on spin 2: the wanted term, $\sigma_{12}(1 + \alpha_1)$, arising from cross relaxation with spin 1 and an unwanted term, $R_2\tau_m$, which arises due to self-relaxation of spin 2 during the mixing time. This latter term must be eliminated as it will give signals in the final spectrum which do not arise from cross relaxation.

This contribution can be eliminated by difference spectroscopy, just as in the conventional transient NOE experiment. A second transient is recorded in which the spin-1 magnetization is not inverted, but in which otherwise everything else is the same. In effect, this simply means setting $\alpha_1 = -1$ in Eq. [27], giving the final magnetizations in the reference experiment as

$$\frac{M_{1z}(\tau_m)_{ref}}{M_0} = 1 + \sigma_{12}\tau_m$$

$$\frac{M_{2z}(\tau_m)_{ref}}{M_0} = R_2\tau_m. \quad [28]$$

In words, all that happens is that the magnetization of spin 2 recovers toward equilibrium. The signals from the two transients, represented by Eqs. [27] and [28], are subtracted from one another to give the following expression for the magnetization contributing to the NOE difference spectrum

$$\frac{M_{1z}(\tau_m) - M_{1z}(\tau_m)_{ref}}{M_0} = (1 + \alpha_1)(R_1\tau_m - 1)$$

$$\frac{M_{2z}(\tau_m) - M_{2z}(\tau_m)_{ref}}{M_0} = (1 + \alpha_1)\sigma_{12}\tau_m. \quad [29]$$

Spin 2 now only has contributions arising from cross relaxation with spin 1, which is what is required.

In practice, this difference step is most simply carried out by repeating the experiment with the phase of the first of the 180° selective pulses, S, advanced by 90°. The magnetization which is selected by the gradients has, by definition, experienced this pulse as a refocusing pulse. Therefore, the change in coherence order, p, is ±2, so that advancing the phase of the pulse by 90° causes the selected magnetization to experience a phase shift of 180°; i.e., it changes its sign, which is just what is required. The simplest implementation is thus to use a two-step phase cycle in which the pulse phase goes (0°, 90°) and the receiver reference phase goes (0°, 180°). In practice, this is often extended to four steps, giving the familiar EXORCYCLE phase cycle of (0°, 90°, 180°, 270°) for the pulse and (0°, 180°, 0°, 180°) for the receiver (*13*).

The DPFGSE experiment thus has more in common with the conventional transient NOE experiment than it does with GOESY in that the former pair both involve selective inversion of the magnetization of the target spin and use difference spectroscopy. In contrast, GOESY in effect involves saturation of the magnetization of the target spin and, as gradients are used to select magnetization, no difference spectroscopy is needed.

The key point which makes the DPFGSE experiment superior to the conventional transient NOE experiment is that, for short to moderate mixing times, in the DPFGSE experiment, the difference step involves subtracting two *small* signals from one another. These signals arise from the spin-2 magnetization which recovers from saturation at the start of the mixing time. In contrast, in the conventional transient NOE experiment, the two signals which are subtracted are close to the full intensity, as the magnetization from which they arise is close to equilibrium in both the irradiated and reference spectra. Thus although the DPFGSE NOE experiment does require the computation of a difference spectrum, the signals which need to be eliminated by the difference are small compared to the equilibrium intensities. The difference step is thus not too demanding on spectrometer stability and excellent spectra are much easier to obtain. At longer mixing times, the magnetization from spin 2 approaches its equilib-

rium value and the difference step becomes more demanding; practical solutions to this problem are presented in the next section.

The explicit solution of the Solomon equations gives the following time dependence of the NOE enhancement in the DPFGSE NOE experiment as

$$\eta_{\mathrm{DPFGSE}} = \frac{M_{2z}(\tau_m) - M_{2z}(\tau_m)_{\mathrm{ref}}}{M_0} = \frac{2\alpha_1\sigma_{12}}{\rho}\left\{\exp\left[-(R_1 + R_2 - \rho)\frac{\tau_m}{2}\right] - \exp\left[-(R_1 + R_2 + \rho)\frac{\tau_m}{2}\right]\right\}. \quad [30]$$

To obtain this result, it has been assumed that the initial magnetization of spin 1 in the irradiated spectrum is given by Eq. [26] and in the reference spectrum is $+\alpha_1 M_0$ (rather than M_0 as was the case in the initial rate analysis).

The NOE enhancements in the transient and DPFGSE experiments are in the ratio $(1 + \alpha_1)/2\alpha_1$ which, since α_1 is likely to be close to 1, is $\sim$1. From the point of view of sensitivity, therefore, the two experiments are closely comparable. Unlike the GOESY experiment, we shall see below that molecular diffusion has little effect on the DPFGSE experiment.

Improving Suppression in DPFGSE NOE

In the DPFGSE NOE experiment, it is necessary to introduce a difference step to cancel that part of the magnetization which arises from self-relaxation during the mixing time. If the mixing time is sufficiently short, i.e., $R_i\tau_m \ll 1$, the extent of recovery is small and the difference step is only required to cancel a small signal. However, as the mixing time is increased, the recovered magnetization will become larger and the demands placed on the subtraction step increase.

A simple and highly effective method of limiting the recovery of this magnetization is to apply a nonselective 180° pulse about halfway through the mixing time (*7*). This inverts any magnetization which has recovered so that, for the remainder of the mixing time, relaxation drives the magnetization toward zero. The result is, at the end of the mixing time, the magnetization is smaller than it would have been in the absence of the 180° pulse.

If the recovery of the magnetization is in the linear regime, i.e., $R_i\tau_m \ll 1$, a 180° pulse in the middle of the mixing time will result in the magnetization returning to zero at the end of the mixing time. However, outside this linear region, such a nulling of the magnetization is achieved by placing the 180° pulse in a different position which can be determined in the following way.

For simplicity, we will assume that behavior of the magnetization of the saturated spins (i.e., all spins other than the target) is dominated by their self relaxation and characterized by a rate constant R; cross relaxation is ignored. If the 180° pulse is placed a time $\beta\tau_m$ into the mixing time, where $0 \leqslant \beta \leqslant 1$, the z magnetization at the end of the mixing time is given by

$$\frac{M_z(\tau_m)}{M_0} = 1 + \frac{\exp(-\beta\Lambda) - 2}{\exp[(1 - \beta)\Lambda]}, \quad [31]$$

where $\Lambda = R\tau_m$. This magnetization is nulled, i.e., $(M_z(\tau_m)/M_0) = 0$, when β is given by

$$\beta = \frac{1}{\Lambda}\ln\frac{1}{2}(1 + \exp\Lambda). \quad [32]$$

For short mixing times, such that $\Lambda \ll 1$, this relationship gives the expected result that the null is achieved with $\beta = 0.5$. As Λ increases, the value of β indicated by Eq. [32] is >0.5; i.e., the 180° pulse needs to be placed later in the mixing time.

Of course, no single value of β can null the magnetization when there is a range of relaxation rate constants present or if a range of mixing times is used. However, β can be chosen in such a way that the recovered z magnetization is less than a certain value for a range of values of Λ. For example, for Λ in the range 0 to 1, a value of β of 0.60 will result in z magnetization which is less than $\sim$3% of its equilibrium value. For a wider range of values of Λ, more of a compromise must be struck: in the case that $0 \leqslant \Lambda \leqslant 2$, a choice of $\beta = 0.67$ will keep the recovered z magnetization to less than 10% of its equilibrium value. For comparison, it should be noted that in the absence of the 180° pulse and for $\Lambda = 2$, the z magnetization would have reached almost 90% of its equilibrium value; the improvement obtained by including the inversion pulse is substantial.

It is clear from the above that the only way to make the nulling process independent of the relaxation rate constants and the mixing time is to work in the limit that the recovery of the magnetization is linear in time, that is, $R\tau_m \ll 1$. This limit can be approached by using two or more inversion pulses, spread throughout the mixing time, so that the time during which the magnetization recovers before being inverted is reduced.

To illustrate the improvement obtainable using extra inversion pulses, we will consider the case of two such pulses. There are many ways of placing the two pulses in the mixing time; the one described here is to imagine first that the mixing time is divided into two equal periods and, in analogy with the above, a 180° pulse is placed a time $\beta\tau_m$ from the beginning of the period. The timing sequence is thus

$$[\beta\tau_m\text{—}180°\text{—}(\tfrac{1}{2}-\beta)\tau_m]\,[\beta\tau_m\text{—}180°\text{—}(\tfrac{1}{2}-\beta)\tau_m]$$

$\frac{1}{2}\,\tau_m$ $\frac{1}{2}\,\tau_m$

As before, in the linear region, a null is achieved by placing the 180° pulses in the middle of the two periods, i.e., $\beta = 0.25$, and for longer mixing times, they move to later in their respective periods. The timing can be simplified by noting that the time between the two 180° pulses is always $\tau_m/2$:

$$\beta\tau_m\text{—}180°\text{—}(\tfrac{1}{2}\tau_m)\text{—}180°\text{—}(\tfrac{1}{2}-\beta)\tau_m.$$

With this sequence and for Λ in the range 0 to 1, a value of β of 0.28 will result in z magnetization which is less than $\sim$0.25% of its equilibrium value. For $0 \leqslant \Lambda \leqslant 2$, a choice of $\beta = 0.30$ will keep the recovered z magnetization to less than 1.5% of its equilibrium value. These results are clearly significant improvements on what can be expected from using a single 180° pulse. Further 180° pulses will result in more precise nulling, although in practice the imperfections in conventional pulses may limit the number that may be used. Frequency-modulated pulses, which give precise inversion over a wide bandwidth and are tolerant to inhomogeneity in the radiofrequency field, are excellent choices for these pulses; specific recommendations are made below.

In practice, it is often the case that a particular resonance is the main cause of difficulty in a DPFGSE NOE experiment recorded using a long mixing time. This may be because the resonance is unusually strong, such as a sharp singlet from a methyl group, or because it is near to other resonances which are receiving NOE enhancements. In such cases, it is advisable to alter the value of β in order to achieve the best null of this unwanted signal. A few short experiments usually suffice to find the required value.

If the 180° pulses used in the mixing time are imperfect, it is possible that they may generate transverse magnetization or cause unwanted coherence-transfer steps. As the NOE enhancements are so small, even minor imperfections can become significant, so particular care must be taken when introducing these extra pulses. In the simple DPFGSE NOE experiment, a gradient G_m is used in the mixing time to dephase all but z magnetization; essentially this gradient acts as a homospoil. This existing gradient can be used to suppress unwanted signals caused by 180° pulses used in the mixing time. For example, the gradient can be placed after the 180° pulse, dephasing any coherences generated by the pulse. An alternative, often employed with inversion pulses, is to split the gradient into two parts (not necessarily equal) and apply them in opposite senses either side of the 180° pulse:

$$G_{m,1}\text{—}180°\text{—}\bar{G}_{m,2}. \qquad [33]$$

Care must be taken to ensure that neither of these gradients refocus any of the gradients used in the DPFGSE sequence.

If two 180° pulses are used in the mixing time, each can be bracketed by gradients in the manner of Eq. [33]. However, with four such gradients in the mixing time and four in the DPFGSE sequence, there is the possibility that unwanted coherence-transfer pathways will be ''accidentally'' refocused. A judicious choice of gradient strengths will avoid this problem and specific recommendations are given below. If they are available, gradients in different directions can be used to advantage as these lessen the chance of accidental refocusing.

The inclusion of one or more inversion pulses in the mixing time affects the dynamics of the NOE; however, it will be shown here that *once the difference step is taken into account* there is no net effect on the final NOE spectrum. For simplicity, we will consider a DPFGSE NOE experiment in which there is a single 180° pulse placed in the middle of the mixing time and that the initial rate approximation applies. The experiment as described above involves subtracting two transients, one in which the magnetization of the target spin is inverted at the beginning of the mixing time and one in which this spin is at equilibrium.

In the first transient, there will be a buildup of magnetization on a spin which is cross-relaxing with the target spin. However, halfway through the mixing time, the inversion pulse rotates the magnetization of the target spin back to the equilibrium position. As the magnetization of the target spin no longer deviates from equilibrium, there is no further buildup of magnetization on the enhanced spin. It thus appears that an NOE enhancement has only built up for *half* of the mixing time.

In the second transient, the magnetization of the target spin starts out at equilibrium so there is no buildup of NOE enhancement for the first half of the mixing time. However, once the 180° pulse inverts this magnetization, an NOE enhancement builds up for the second half of the mixing time. So, just as in the first case, the NOE enhancement only builds up for half of the mixing time. Once the difference between the two experiments is computed, the overall effect is as if an NOE enhancement has built up for half the mixing time.

For the simple DPFGSE NOE experiment with *no* inversion pulse in the mixing time, an NOE enhancement builds up for the entire duration of the mixing time for the first transient in which the magnetization of the target spin is inverted. For the second transient, in which the magnetization of the target spin is at equilibrium, no NOE enhancement builds up. Again, when the difference is computed, the effect is as if an enhancement has built up for half the mixing time. Thus, DPFGSE experiments with and without the 180° pulse in the mixing time yield identical enhancements.

A full calculation in which the initial rate is not assumed and in which the inversion pulse is not placed in the middle of the mixing time leads to the same conclusions. The

buildup of the NOE enhancements is thus unaffected by the inclusion of nonselective-inversion pulses in the mixing time.

Diffusion

Molecular diffusion will cause a loss of signal intensity in any experiment in which magnetization is dephased by one gradient and then subsequently rephased by a second. The effect arises because for complete refocusing the phase induced by the second gradient must be equal and opposite to that induced by the first. Thus, as the phase is spatially dependent, complete refocusing will only be achieved if the spins do not move.

For a simple spin echo with gradients placed either side of the 180° pulse the signal, A, in the presence of diffusion compared to that in the absence of diffusion, A_0, is given by the well-known relationship (*14*)

$$\frac{A}{A_0} = \exp(-\gamma^2 G^2 \delta^2 \Delta D), \qquad [34]$$

where D is the self diffusion constant, γ is the gyromagnetic ratio, G is the strength if the magnetic field gradient (e.g., in tesla per meter, assumed to be in one direction), δ is the duration of the gradients, and Δ is the time between the start of the two gradients; it is assumed that $\Delta \gg \delta$. This relationship embodies the idea that the larger the phase induced by the gradient, that is, the longer or stronger the gradient becomes, the more rapidly the signal is attenuated. Also the more rapid the diffusion of the molecules, reflected by a larger D, the more rapidly the signal is attenuated. Finally, the time separation, Δ, of the two gradients is important as it is mainly during this time that diffusion of the phase-labeled spins will take place.

The expression of Eq. [34], while not applying exactly to either the GOESY or DPFGSE NOE experiments, can be used as a guide to the size of the expected effects. In GOESY, the key point is that the first set of gradients, which together dephase the wanted magnetization, are separated from the final refocusing gradient by the mixing time, and as this time can easily be a second or more, there is a substantial period during which diffusion can take place. For example, for a molecule in a nonviscous solvent, such as $CDCl_3$, a spin echo consisting of two 1.5 ms gradients, of strength 10 G cm^{-1} and separated by 0.5 s, less than 15% of the magnetization is refocused at the end of the echo; this is a serious loss of signal. In contrast, in the DPFGSE NOE experiment, the magnetization of the target spin is refocused at the end of the excitation sequence, and there is no gradient after the mixing time. The losses due to diffusion will thus be very much smaller than for GOESY and will also be independent of the mixing time.

Explicit expressions for the diffusion losses in the GOESY and DPFGSE NOE experiments can be calculated by the same method used to derive Eq. [34]. For GOESY the signal, A_{GOESY}, is given by

$$\ln \frac{A_{\mathrm{GOESY}}}{A_{\mathrm{GOESY},0}} = -D\gamma^2 \left[\begin{array}{l} \frac{\delta^3}{3}(40G_1^2 + 40G_1G_2 + 16G_2^2) \\ +\delta^2 t_{\mathrm{p}}(5G_1^2 + 4G_1G_2 + G_2^2) \\ +4\delta^2\tau_{\mathrm{m}}(G_1^2 + 2G_1G_2 + G_2^2) \end{array} \right], \qquad [35]$$

where G_1 and G_2 are the strengths of the gradients placed as shown in Fig. 2a, δ is the length of the gradients (assumed to all be the same), and t_{p} is the duration of the selective pulses in the excitation sequence. G_3 is set to refocus the four gradients in the excitation sequence, i.e., $G_3 = 2(G_1 + G_2)$. The corresponding signal from the DPFGSE NOE sequence, A_{DPFGSE}, is

$$\ln \frac{A_{\mathrm{DPFGSE}}}{A_{\mathrm{DPFGSE},0}} = -D\gamma^2 \left[\begin{array}{l} \frac{2\delta^3}{3}(G_1^2 + G_2^2) \\ +\delta^2 t_{\mathrm{p}}(G_1^2 + G_2^2) \end{array} \right]. \qquad [36]$$

Note that in comparison to the expression for A_{GOESY}, there is no dependence on the mixing time. In the case of GOESY, a simpler and more usable expression can be found by assuming that $\tau_{\mathrm{m}} \gg \delta$, t_{p} and that $G_1 = G_2 = G$:

$$\ln \frac{A_{\mathrm{GOESY}}}{A_{\mathrm{GOESY},0}} \approx -D\gamma^2(16G^2)\delta^2\tau_{\mathrm{m}}. \qquad [37]$$

As each of the gradients G_1 and G_2 appear twice (see Fig. 2a), the total dephasing is equivalent to a single gradient of strength $4G$. The expression for a simple spin echo, Eq. [34], thus translates directly to the approximate expression for A_{GOESY} with the identification $G \rightarrow 4G$ and $\Delta \rightarrow \tau_{\mathrm{m}}$.

Figure 3 shows the signal losses predicted by Eqs. [35] and [36] for a typical set of experimental parameters. As expected, the loss of signal in the DPFGSE NOE experiment is negligible, even for a low viscosity solvent such as $CDCl_3$. In contrast, the losses in GOESY are severe. For a nonviscous solvent, it is seen that 50% of the signal is lost for a mixing time of around 150 ms; after 0.5 s, virtually all the signal is lost. For a more viscous solvent, such as D_2O, the situation is somewhat better, but there is still a significant loss of intensity for even modest mixing times.

The amount of magnetization lost due to diffusion during the GOESY experiment can be minimized by reducing the length and strength of the field gradient pulses. However, there is a limit to the extent to which this can be taken, as a certain minimum amount of dephasing is needed to achieve

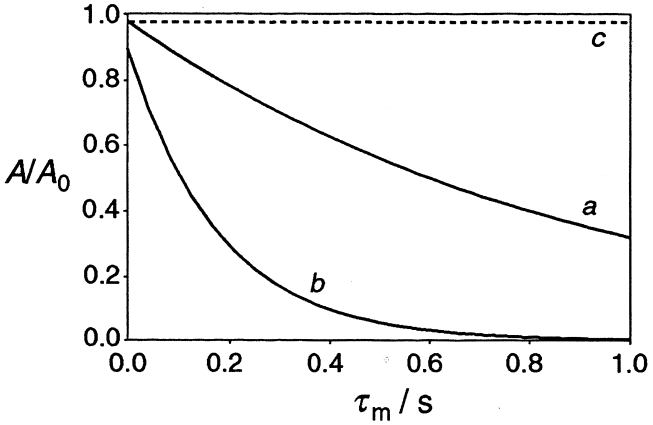

FIG. 3. Plots showing the calculated signal loss, as a function of mixing time, due to the effects of diffusion on the GOESY and DPFGSE NOE experiments, whose pulse sequences are shown in Fig. 2. The signal is expressed as a fraction of that expected in the absence of diffusion; relaxation and pulse imperfections are ignored. Curve (a) is calculated for a GOESY experiment in a nonviscous solvent, such as $CDCl_3$, with a diffusion constant, D, of 2.5×10^{-9} m^2 s^{-1}, and curve (b) is calculated for a more viscous solvent, such as water, with a diffusion constant, D, of 0.5×10^{-9} m^2 s^{-1}. The dashed line (c) is calculated for the DPFGSE NOE experiment; there is no visible difference on the plot between the lines for a viscous and nonviscous solvent. The duration of the gradient pulses and the selective pulses have been taken as 1 and 25 ms, respectively. The strength of the gradient G_1 has been taken as 0.05 T m^{-1} (5 G cm^{-1}), the gradient G_2 has been taken as 0.75 times the strength of G_1, and in the GOESY experiment, the gradient G_3 has been set to the value needed to refocus the combined effects of the dephasing gradients G_1 and G_2.

the required suppression of unwanted resonances. An additional problem arising from diffusion in a GOESY experiment is that the observed time dependence of the NOE enhancement is affected not only by the relaxation rate constants but also by diffusion processes. As a result, the value of the initial slope, measured from the linear region of the NOE buildup curve, is affected by diffusion, and in addition, the duration of the linear region is curtailed. Thus, if quantitative comparisons are to be made it is essential that the buildup curves are all measured using the same values for the length and strength of the gradients and the same length for the selective pulses.

In contrast, in the DPFGSE experiment, the losses due to diffusion do not increase with increasing mixing time, and so the buildup curves are not falsified. It is clear that for molecular systems in which spatial diffusion is significant, the DPFGSE sequence is to be preferred.

SPT AND ZERO-QUANTUM INTERFERENCE EFFECTS

NOE spectra of all kinds are frequently plagued by what are loosely called ''SPT artifacts'' (*3, 15*). These are multiplets which have anti-phase character in them, that is multiplets with both positive and negative lines. Most often the lines of such multiplets have complex patterns of phase and intensity indicating contributions from of a number of different anti-phase terms, such as $2I_{1x}I_{jz}$ or $4I_{1x}I_{jz}I_{kz}$. As these terms have a variety of origins, we shall describe them as ''anti-phase contributions'' to the NOE spectrum.

In principle, as these anti-phase contributions all have zero integral across the multiplet, their presence does not prevent the interpretation of NOE spectra as inspection of the integral should reveal those multiplets which have an NOE enhancement. However, in practice, it is often difficult to decide whether a small integral is indicative of an NOE enhancement or is simply due to deficiencies in the integration process. In addition, if there is overlap between multiplets which have anti-phase contributions, it can become difficult to interpret the integral. Anti-phase contributions are also unaesthetic and can confuse the inexperienced. For all these reasons, therefore, it is very desirable to eliminate these contributions.

Typically, the anti-phase contributions are not large, amounting to perhaps a percent or two of the equilibrium intensity, and ordinarily they would be regarded as quite negligible. However, as the NOE enhancements we wish to measure are frequently very small, even such tiny anti-phase contributions are significant. They need, therefore, to be suppressed to very low levels, a task which is challenging as at these low levels the anti-phase terms result from what would normally be regarded as minor imperfections of the pulses.

In the GOESY or DPFGSE NOE experiment, anti-phase contributions in the spectra arise from two types of terms present during the mixing time: zero-quantum coherence and what we shall call ''*zz* terms'' (operators such as $2I_{1z}I_{2z}$ and $4I_{1z}I_{2z}I_{3z}$). Both of these have coherence order zero and so are not suppressed by the purging gradient, G_m, applied during the mixing time, and both can be converted to observable anti-phase terms by the final nonselective pulse. We shall consider first how such terms arise and then how they can be suppressed.

It has already been described in a previous section how anti-phase terms may be generated by the selective-excitation sequence. Some of these terms can be turned into zero-quantum coherence by the nonselective 90° pulse at the start of the mixing time

$$2I_{1x}I_{2z} \xrightarrow{\frac{\pi}{2}F_x} -2I_{1x}I_{2y}$$

$$4I_{1y}I_{2z}I_{3z} \xrightarrow{\frac{\pi}{2}F_x} 4I_{1z}I_{2y}I_{3y}, \qquad [38]$$

where $F_x = \Sigma_i I_{ix}$; the terms on the right in Eq. [38] all contain zero-quantum contributions. A perfect 90° pulse cannot generate *zz* terms, but in practice the combination of pulse miss-set, B_1 inhomogeneity and off-resonance effects result in the generation of such terms. Imperfect pulses can also lead to the generation of other kinds of zero-quantum coherence, such as $2I_{1x}I_{2x} + 2I_{1y}I_{2y}$. Also, if the selective excitation is less than perfect, anti-phase terms on other spins may be present, and these can also give rise to zero-quantum coherence. All of these unwanted terms can be minimized by optimization of the selective excitation as described in an earlier section.

During the mixing time, these zero-quantum coherences evolve so in general just prior to the final nonselective 90° pulse there is a mixture of all possible zero-quantum operators. The 90° pulse at the end of the mixing time generates observable anti-phase magnetization from parts of some of these terms, for example,

$$\mathrm{ZQ}_{12,y} \equiv 2I_{1y}I_{2x} - 2I_{1x}I_{2y} \xrightarrow{\frac{\pi}{2}F_x} 2I_{1z}I_{2x} - 2I_{1x}I_{2z}$$

$$\mathrm{ZQ}_{12,x} \equiv 2I_{1x}I_{2x} + 2I_{1y}I_{2y} \xrightarrow{\frac{\pi}{2}F_x} 2I_{1x}I_{2x} + 2I_{1z}I_{2z}$$

$$4I_{1z}I_{2x}I_{3x} + 4I_{1z}I_{2y}I_{3y} \xrightarrow{\frac{\pi}{2}F_x} -4I_{1y}I_{2x}I_{3x} - 4I_{1y}I_{2z}I_{3z}. \quad [39]$$

In contrast, the 90° pulse converts *zz* terms into multiple-quantum coherence and no observable signals are generated.

However, the 90° pulse at the end of the mixing time cannot be assumed to be perfect and as a result *zz* terms do lead to observable signals, as do all kinds of zero-quantum coherence. In addition, if there are extra 180° pulses, either as nulling pulses in the mixing time in the DPFGSE NOE experiment, or after the final 90° pulse as in the GOESY experiment, there exists the possibility of further coherence transfers.

In practice, we have found that, although anti-phase contributions can be minimized by careful adjustment of the excitation sequence they often remain strong enough to swamp small NOE enhancements. This is particularly a problem when making measurements at short mixing times or when long-range enhancements are being sought. Anti-phase contributions are also particularly troublesome when there is markedly unequal excitation of the lines in the target multiplet either because it is wide, due to the presence of many couplings, or because spectral crowding requires the use of very selective excitation.

We have found that a simple and effective way of reducing the level of the anti-phase contributions is to apply, at the *end* of the mixing time and on alternate transients, a selective-inversion pulse to the target spin; the receiver phase is held constant. In practice, it is usual to implement this method by always applying the selective pulse but with the transmitter carrier moved outside the spectral region on alternate transients. Thus, the selective pulse goes {on, off} and the receiver continues to add the signals. In the DPFGSE NOE experiment, this extra step is in addition to the four steps of EXORCYCLE, resulting in a basic eight-step phase cycle.

The effect of this 180° pulse is to change the sign of any *zz* terms that are present at the end of the mixing time and so change the sign of any contribution that these terms make to the spectrum, thus leading to their cancellation. A side effect of the inclusion of the pulse is that the signal from the target spin disappears from the final spectrum, since the corresponding magnetization is inverted by the pulse.

The effect of this selective-inversion pulse on the zero-quantum terms is more complex: for example,

$$\mathrm{ZQ}_{12,y} \equiv 2I_{1y}I_{2x} - 2I_{1x}I_{2y} \xrightarrow{\pi I_{1x}} -2I_{1y}I_{2x} - 2I_{1x}I_{2y}$$

$$\mathrm{ZQ}_{12,y} \equiv 2I_{1y}I_{2x} - 2I_{1x}I_{2y} \xrightarrow{\pi I_{1y}} 2I_{1y}I_{2x} + 2I_{1x}I_{2y}$$

$$\mathrm{ZQ}_{12,x} \equiv 2I_{1x}I_{2x} + 2I_{1y}I_{2y} \xrightarrow{\pi I_{1x}} 2I_{1x}I_{2x} - 2I_{1y}I_{2y}$$

$$\mathrm{ZQ}_{12,x} \equiv 2I_{1x}I_{2x} + 2I_{1y}I_{2y} \xrightarrow{\pi I_{1y}} -2I_{1x}I_{2x} + 2I_{1y}I_{2y}. \quad [40]$$

From Eq. [40], it is seen that only one of the operator products which contributes to each zero-quantum term changes sign, and which product this is depends on the phase of the 180° pulse. The situation is further complicated by the fact that the contribution to the final spectrum of the different operator products depends on the precise form of the final 90° pulse, i.e., the nature of any imperfections. The expectation is that there will be a significant, but not complete, suppression of the anti-phase terms which arise from zero-quantum coherence.

If the suppression obtained by this method is still insufficient, further improvement can be obtained by adding a second selective 180° pulse. The two selective pulses are applied on or off resonance in two independent steps to give the four-step cycle

$$\{\text{on, off, on, off}\}_{\text{pulse 1}}\{\text{on, on, off, off}\}_{\text{pulse 2}}.$$

These selective pulses are sufficiently long that there will be some evolution of the coherences present and so a term affected in one way by the first inversion pulse may well be affected differently by the second. Thus the combined effect of the two pulses is greater than either on its own.

Figure 4 compares NOE spectra of 6(5H)-phenanthridinone, **1,** recorded using the simple DPFGSE NOE experiment, with spectra recorded using one or two selective 180° pulses at the end of the mixing time; a series of spectra at increasing mixing times is shown. The spectra recorded using the simple sequence show substantial anti-phase contributions, which obscure the underlying enhanced multiplets, even for mixing times as long as 250 ms. Adding one selective 180° pulse gives a major improvement, revealing the underlying enhanced multiplet with near to the correct pattern of intensities within the multiplet. However, at the shorter mixing times there is still some distortion visible. The use of two selective 180° pulses gives a further substantial improvement which is especially evident at short mixing times. The maximum NOE enhancement of H_6 shown in these spectra is just 2%, so it is clear that the inclusion of the selective 180° pulses has reduced the anti-phase contributions to a very low level.

Figure 5 compares NOE buildup curves of **1** recorded using the DPFGSE NOE experiments without and with one or two selective 180° pulses in the mixing time. The NOE enhancements have been quantified by careful integration of the enhanced multiplets. It is clear that the presence of anti-phase contributions to the spectra leads to considerable scatter on the plots; this is particularly so at short mixing times. However, with the inclusion of two 180° pulses [plots (c) and (f)], the scatter is largely eliminated. Careful analysis of the buildup curves in (c) and (f) gives the ratio of the cross-relaxation rate constants between H_5 and H_4 and between H_6 and H_4 as 1.00 ± 0.07; this translates to a ratio of distances of 1.00 ± 0.01. It should be noted that although the presence of the extra 180° pulses results in an unknown but constant shift in the mixing-time origin, the slope of the buildup curve is unaffected.

Generally, interference from anti-phase contributions is only likely to be a problem at short mixing times when the NOE enhancements are small. At longer mixing times not only are the NOE enhancements larger but also it is often the case that the terms giving rise to anti-phase contributions will have decayed away due to relaxation. The result is that the NOE enhancements dominate and so the measures described in this section are not necessary.

Strong Coupling

It has been assumed in the discussion so far that the spins involved are weakly coupled. If this assumption is relaxed, the analysis and interpretation of the NOE experiments becomes much more complex (*1, 16*). The situation which is most likely to be of practical interest is one in which the target multiplet shows evidence of a small degree of strong coupling, i.e., it is roofed, but that the multiplets of the strongly coupled spins are sufficiently separated that selective excitation of just one of them is feasible. It will be shown in this section that in such a situation there will be anti-phase contributions in the NOE spectrum *even when the pulses are perfect.* These contributions therefore result from the strong coupling in the spin system. However, it will be shown that the procedure described in the previous section suppresses them to a significant degree.

We shall confine our analysis to a strongly coupled system of two spins, A and B. The degree of strong coupling can be expressed by the strong coupling parameter, tan 2θ, defined as

$$\tan 2\theta = \frac{J_{AB}}{\upsilon_A - \upsilon_B}, \qquad [41]$$

where υ_i is the offset (in hertz) of spin i and J_{AB} is the coupling (in hertz) between spins A and B; θ is defined to fall in the range $\pm\pi$ and takes a unique value which can be found by inspecting the signs of J_{AB} and $(\upsilon_A - \upsilon_B)$ separately. The limit of weak coupling corresponds to $\theta = 0$ and when the two shifts are degenerate $|\theta| = \pi/4$. The four energy levels of this spin system have wave functions which can be expressed as linear combinations of the product functions

$$|1\rangle = |\alpha\alpha\rangle \quad |2\rangle = \cos\theta|\alpha\beta\rangle + \sin\theta|\beta\alpha\rangle$$
$$|3\rangle = \cos\theta|\beta\alpha\rangle - \sin\theta|\alpha\beta\rangle \quad |4\rangle = |\beta\beta\rangle, \qquad [42]$$

where the notation $|\alpha\beta\rangle$ implies spin A in spin state α and spin B in spin state β, etc.

The conventional spectrum of two such strongly coupled spins consists of four lines in the familiar roofed pattern; the two inner lines have intensity $(1 + \sin 2\theta)$, whereas the two outer lines have intensity $(1 - \sin 2\theta)$. For modest degrees of strong coupling, the two transitions between levels 1 and 3 and between 2 and 4 can be thought of as mainly due to transitions of spin A. Likewise, transitions 1–2 and 3–4 can be associated primarily with spin B. Figure 6a shows how the intensities of these transitions vary with θ, and Fig. 6b shows, for $\theta = 0.1$, the usual spectrum displaying the characteristic AB pattern. As was commented on above, only modest degrees of strong coupling are of practical interest here; hence, only relatively small values of θ are considered.

The transient NOE experiment, involving applying a selective 180° pulse to the pair of transitions associated mainly with spin A, is the simplest to analyze; relaxation effects will be ignored in the calculation so that the underlying effects due to strong coupling can be isolated. In addition, evolution of coupling *during* the pulse is ignored. Figure 6c shows the intensity of the four lines in the NOE difference

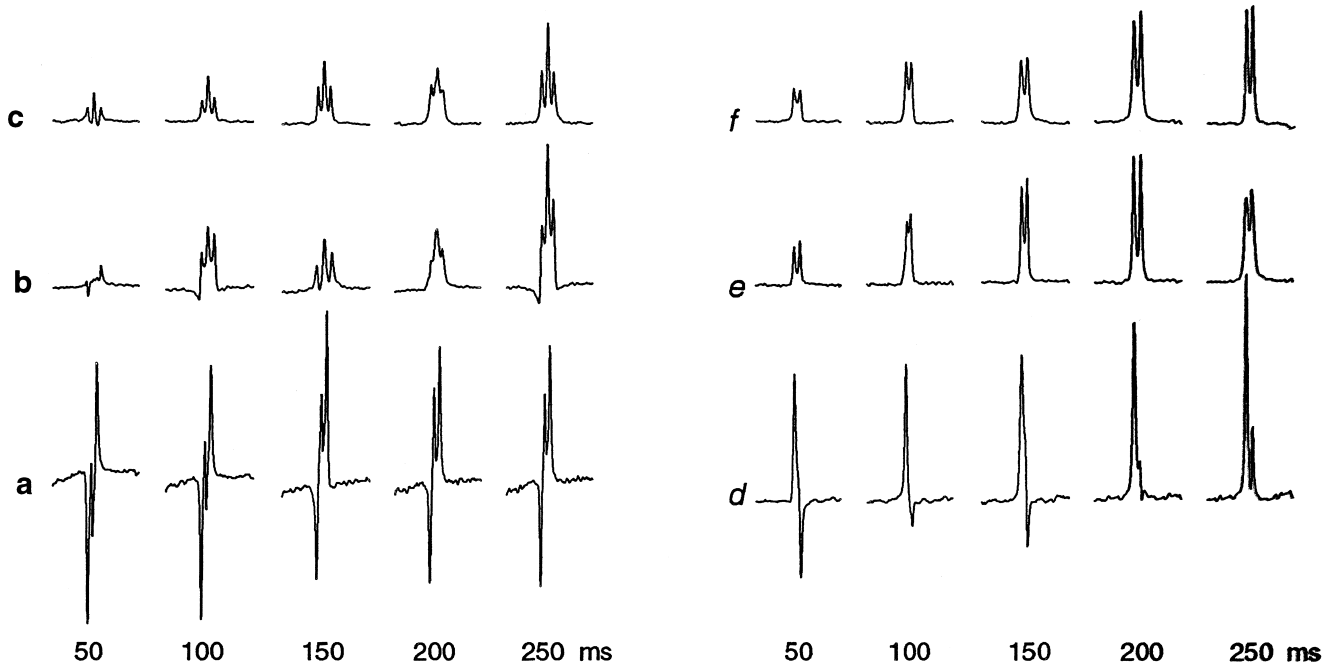

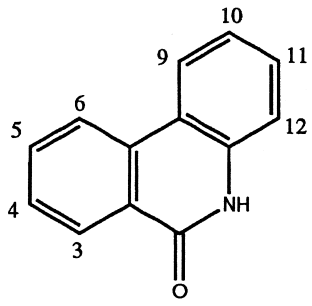

1

FIG. 4. DPFGSE NOE spectra of 6(5H)-phenanthridinone, **1** (structure and numbering shown); in all cases H_5 was the target. Spectra (a)–(c) show the enhanced multiplet from H_4 and spectra (d)–(f) show the enhanced multiplet from H_6; a series of spectra recorded with different mixing times are shown. Spectra (a) and (d) were recorded using the simple DPFGSE NOE sequence of Fig. 2a; they show substantial anti-phase contributions which obscure the underlying enhanced multiplet. Spectra (b) and (e) were recorded with the modified sequence, described in the text, in which a selective 180° pulse is added at the end of the mixing time; there is clearly a substantial reduction in the anti-phase contributions, although at the shortest mixing times there is still evidence of some distortions of the multiplet structures. Spectra (c) and (f) were recorded using a sequence with two selective 180° pulses added at the end of the mixing time (see text for details). These spectra show a further improvement over those shown in (b) and (e), and the lines of the multiplet have close to their correct relative intensities for all mixing times. Spectra were recorded at 500 MHz for protons; the selective pulses were all shaped to a Gaussian truncated at the 1% level and of duration 40 ms. The gradients were all of duration 1 ms, and G_1 and G_2 were of strength 20 and 12% of full power (10% is approximately 3.8 G cm^{-1}). For spectra (b) and (e), the selective 180° pulse was accompanied by the gradient sequence $G_{m,1}$—180°—$\bar{G}_{m,2}$; both gradients were of duration 1 ms and strength 7 and −6% of full power respectively (the minus sign indicates a gradient applied in the opposite direction). For spectra (c) and (f), the two selective 180° pulses were accompanied by the gradient sequence $G_{m,1}$—180°—$\bar{G}_{m,2}$—180°—$G_{m,3}$ where the gradients were the same length as before and of strength 7, −11, and 4% respectively. The sample concentration was approximately 10 mM in DMSO-d_6.

spectrum, calculated for zero mixing time and using these approximations, plotted as a function of θ. It is clear from the plot that as the degree of strong coupling increases the two lines associated mainly with spin B show an increasing anti-phase contribution. The plot also shows that for even the modest degree of strong coupling characterized by θ =

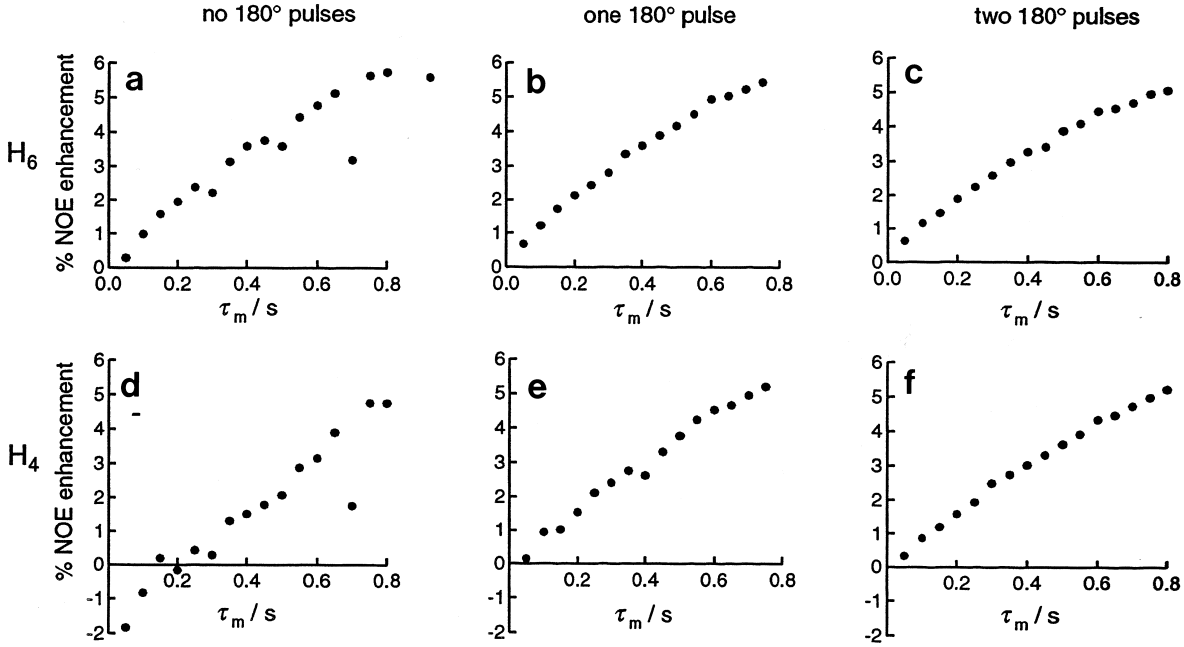

FIG. 5. NOE enhancement buildup curves from spectra of 6(5H)-phenanthridinone in which H_5 was the target. Plots (a)–(c) are of the enhancement of H_6, while (d)–(f) are for H_4. For plots (a) and (d), the simple DPFGSE experiment was used, a single selective 180° pulses was added to record the data shown in plots (b) and (e), and two such pulses were used to record the data shown in plots (c) and (f). The presence of anti-phase contributions in the spectra recorded using the first two sequences leads to scatter on the data, but this is largely eliminated by using the final sequence. The fractional enhancements were estimated by the method described in the text; experimental details are as described in the legend to Fig. 4.

0.1, the anti-phase contribution is significant, amounting to 10% or so of the equilibrium intensity. Figure 6d shows the NOE difference spectrum expected for $\theta = 0.1$.

The details of the calculation reveal that part of the origin of these anti-phase contributions is zero-quantum coherence which is generated by the selective 180° pulse. In weakly coupled spin systems, a single pulse applied to a spin system at equilibrium does not generate any zero-quantum coherence. However, in the presence of strong coupling, coherences of order zero can be generated. The nonselective 90° pulse transfers this zero-quantum coherence to observable single quantum, giving rise to the anti-phase contributions.

If evolution of the coupling during the pulse is included in the calculation, or if the zero-quantum coherence is allowed to evolve during a finite mixing time, the lines associated with spin B acquire mixed phases. The absolute intensity of the contributions to these B spin lines is approximately the same as that predicted by the simple calculation.

Figure 7 shows a series of AB spectra, with increasing degree of strong coupling, and the resulting NOE difference spectra recorded using the conventional transient NOE experiment. A frequency-dependent phase correction has been used to adjust the phase of the lines mainly associated with the B spin so that the anti-phase contribution is most evident. The intensities of these lines are in approximate agreement with the predictions of the simple theory described above.

The method for suppressing anti-phase contributions which was described in the previous section is also quite successful at suppressing such contributions associated with strong coupling. The degree of suppression that can be expected varies with the phase that the zero-quantum coherence acquires during the mixing time. Depending on this phase, the suppression can vary between complete and 50%. As before, two selective 180° pulses, especially if separated by a time comparable with the period of the evolution of the zero-quantum coherence, give even better suppression.

PRACTICAL ASPECTS

Recommendations

As has been described above, the GOESY experiment suffers from a significant loss of signal due to diffusion during the mixing time, an effect which is especially severe for commonly used nonviscous solvents such as chloroform. Therefore, our recommendation for general use is the DPFGSE NOE sequence with the addition of one or two nonselective inversion pulses in the mixing time. If anti-phase contributions are a problem, one or two selective inversion pulses should be added at the end of the mixing time, in the way described above. Pulse sequences with detailed timing diagrams are shown in Fig. 8.

It is usually recommended that each gradient pulse be followed by a short delay to allow the spectrometer and the

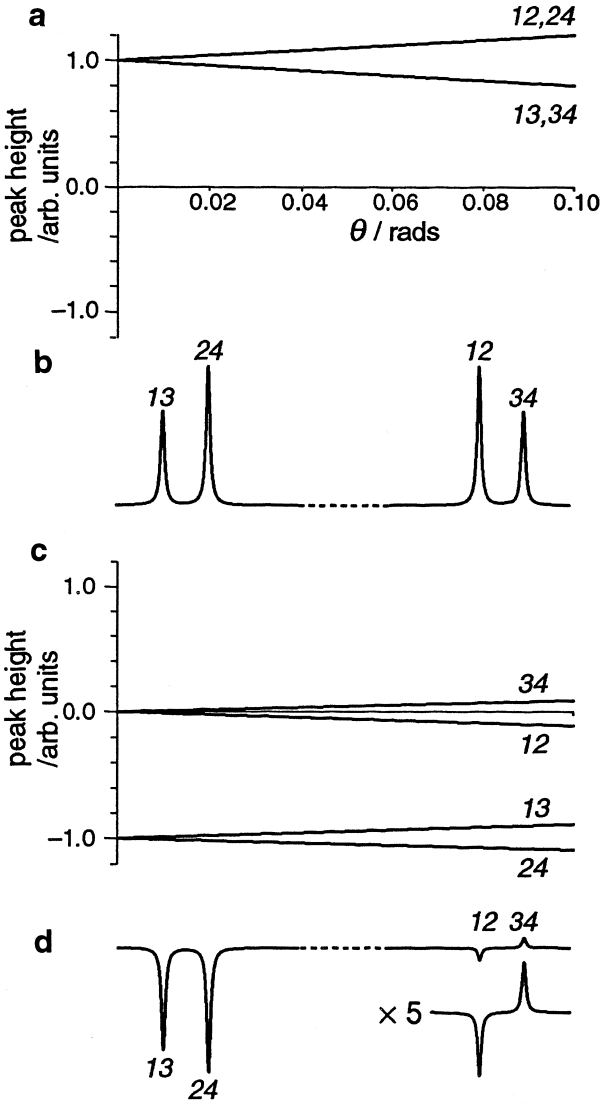

FIG. 6. Simulations showing the effect of strong coupling on NOE spectra. Plot (a) shows how the intensity of the two inner lines (transitions 1–2 and 2–4), and two outer lines (1–3 and 3–4) of the normal spectrum from a strongly coupled AB system varies with degree of strong coupling, expressed by the parameter θ which is defined in Eq. [41]. Shown in (b) is the AB spectrum calculated for $\theta = 0.1$. Plot (c) gives the intensities of the four lines in the conventional transient NOE spectrum in which the selective inversion pulse is applied to the two transitions 1–3 and 2–4 which are mainly associated with the A spin. As the extent of strong coupling increases, the multiplet associated with the B spin, transitions 1–2 and 3–4, acquires an anti-phase contribution. Shown in (d) is the NOE difference spectrum expected for $\theta = 0.1$. In all of these plots, the intensity has been normalized so that the lines in the weakly coupled spectrum have intensity 1.0.

field-frequency lock to recover. Such delays are included in the sequences shown in Fig. 8. We have found that the best results are obtained by maintaining complete symmetry in the double-echo sequence, so identical delays, d, are included prior to each gradient. The switching of field-frequency lock stabilizing circuits and power levels can also be accomplished during these delays.

The DPFGSE sequence lends itself very well to a convenient method of pulse calibration and assessment of degree of selectivity. A simple experiment is run in which a nonselective 90° pulse is followed by the DPFGSE sequence (that is, all pulses up to point A in Fig. 8a); the selective pulses are on resonance with the desired target. Since this sequence will give the maximum signal when the two selective elements, S, are closest to inversion pulses, pulse calibration can easily be achieved by varying the length, power, or other parameters that describe S in order to give the maximum signal. As the phase of the signal produced is independent of the form of S, it is easy to identify the maximum. This procedure is particularly convenient for frequency-modulated pulses which can be difficult to calibrate in more conventional ways.

Once the pulse is calibrated, the spectrum can be examined to check that the selective excitation is satisfactory, i.e., that it is sufficiently narrowband and that the target multiplet has been excited uniformly. The parameters which describe the selective pulses can be altered to improve any unsatisfactory aspects of the excitation. Once the DPFGSE sequence is calibrated, the parameters can be transferred directly to the NOE sequence and then used without further adjustment.

Essentially any pulse can be used for the selective element S. Since in the DPFGSE sequence the phase properties of S are not important, it is only necessary to select S on the basis of its inversion profile. In addition, as the selectivity of the DPFGSE sequence ultimately depends on the square of the inversion profile of S, the pulse need not be as selective as would be required if it were used on its own.

A Gaussian-shaped pulse is the simplest choice for the soft pulses S and S_m. The truncation level can be set as high as 10–20% as any ''sinc wiggle'' type excitation outside the main bandwidth is highly attenuated by the multiplicative action of the DPFGSE. There is a slight disadvantage in that losses due to pulse miscalibration or spatial inhomogeneity of the B_1 field are also multiplicative, leading to less-than-perfect inversion of the target, with 70% signal retention being typical. The inversion bandpass is also not completely uniform for a wide multiplet, which is not desirable. A unique feature of the DPFGSE method, though, is that *any* inversion pulse can be used for S; the phase properties of the pulse are unimportant, and all lines of the multiplet will be excited with the same phase. Waveforms with a hyperbolic secant amplitude profile and with a hyperbolic tangent frequency sweep (*17, 18*) are known to have inversion profiles that are nearly independent of the B_1 field strength once a threshold is reached, and might be thought to be ideal candidates to avoid any signal loss. However, these inversion pulses are *adiabatic* (*17*) and hence necessarily require rather longer to implement for a given selectivity, resulting is losses due to transverse relaxation. In addition, the higher

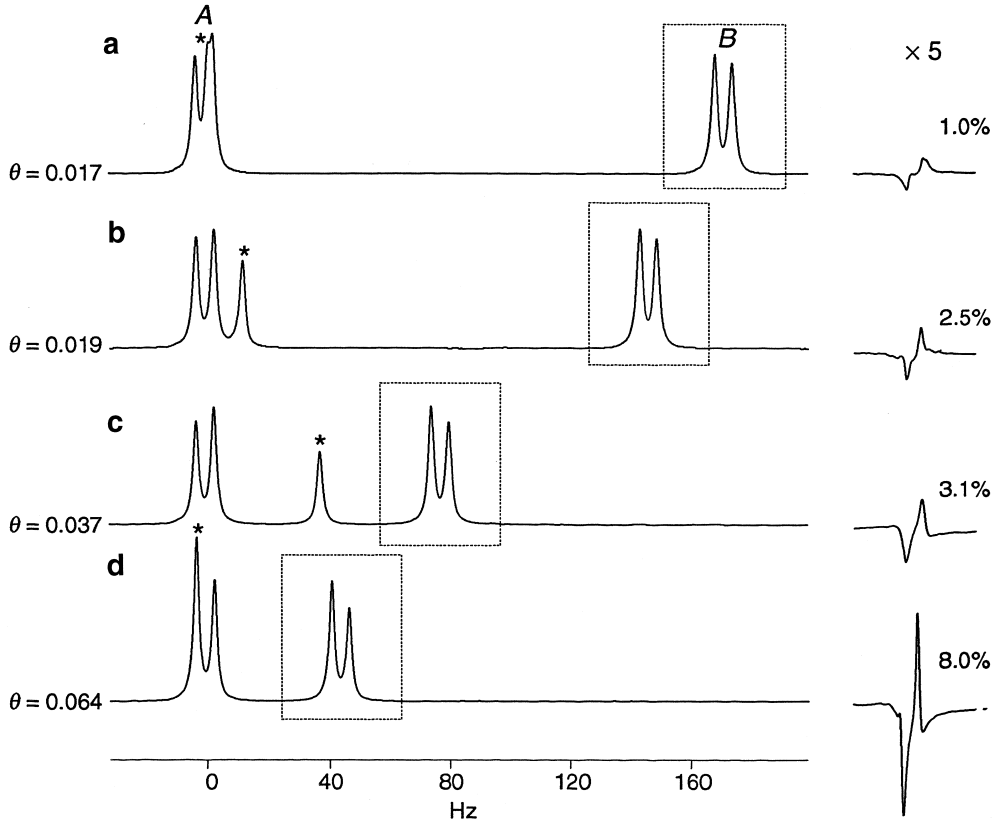

FIG. 7. Experimental spectra of 2,3-dibromothiophene showing the effects of increasing degrees of strong coupling on transient NOE spectra. The degree of strong coupling is different in the spectra (a)–(d) and is indicated by the value of θ shown on the left. The complete AB spectrum is plotted, and to the right is shown the B spin multiplet (indicated by the box) taken from the NOE difference spectrum; the NOE spectra have been phased so that the lines of the A multiplet are negative. The anti-phase contributions are easily seen and their intensities are in approximate agreement with the plots shown in Fig. 6c. The degree of strong coupling was varied by titrating C_6D_6 into a sample made up initially in $CDCl_3$; the lines denoted $*$ are from impurities. The selective 180° pulse was 40 ms in duration and was shaped to a Gaussian truncated at the 1% level.

peak power required during the pulse can perturb nearby coupled spins significantly, possibly leading to the production of more zero-quantum coherence. For these reasons, we have designed some new frequency-modulated pulses which are *not* adiabatic but which show some tolerance to B_1 inhomogeneity. Figure 9 shows the phase and amplitude profile of one such band-selective pulse, which we name ''son2''[1]; for comparison, a linear frequency sweep would give a purely quadratic phase function. Thus, the frequency profile of this selective pulse is somewhat novel, changing directions several times. Such pulses have other interesting properties, which will be explored elsewhere.

There are any number of good choices for the broadband inversion pulse, S_{null}, used in the mixing time; here the main criterion is highly accurate spin inversion over the whole proton shift range. At high fields, conventional 180° pulses do not give good inversion over the full proton shift range, even when the highest practicable radiofrequency field strength of around 30 kHz is used. There are a number of inversion pulses which are more effective than the simple pulse; for example, composite pulses of the type $90^\circ_x 240^\circ_y 90^\circ_x$ (*19*), the GROPE-16 pulse (*20*) or conventional hyperbolic secant inversion pulses applied at full power (*17*). A particularly good compromise between brevity, peak power, and inversion accuracy can be achieved by the nonlinear frequency-modulated pulse shown in Fig. 10 (see footnote 1). This pulse achieves near-perfect inversion over a 15 kHz bandwidth (easily sufficient to cover the entire proton shift range at the highest fields), and the pulse is tolerant to deviations of the radiofrequency field strength by up to ±30% of its nominal value; these desirable properties are achieved in just 192 μs and with a peak radiofrequency field strength of just 15.6 kHz. This pulse is six times longer than a conventional 180° pulse of the same peak power but has much better inversion performance than the composite pulse $90^\circ_x 240^\circ_y 90^\circ_x$, and better performance than GROPE-

[1] Details of how the profiles of this pulse can be downloaded are to be found on the Web page http://www.chem.uci.edu/research/faculty/ajshaka.html.

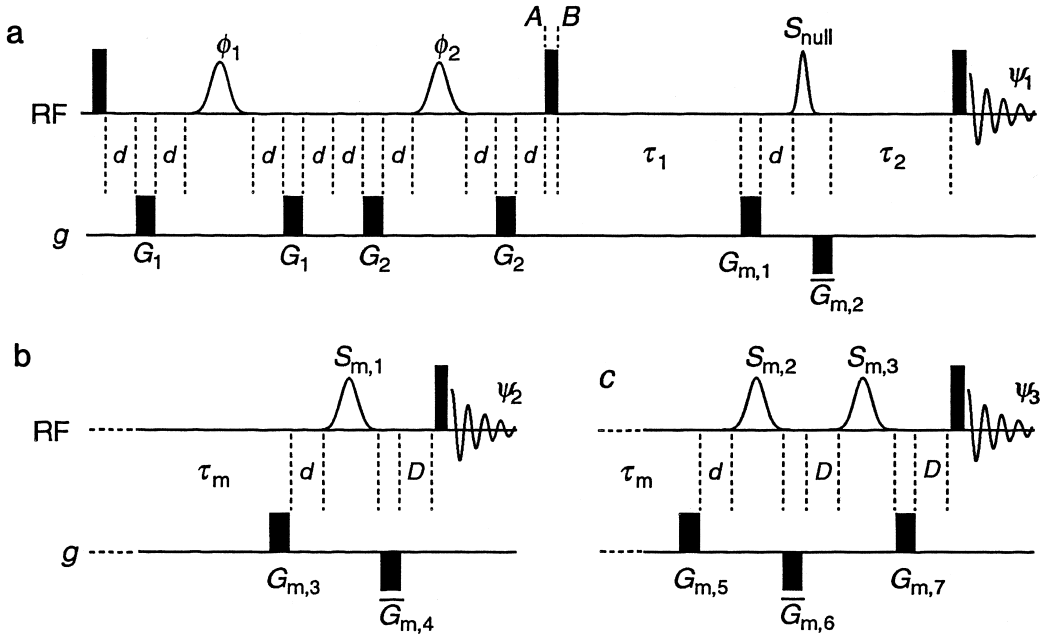

FIG. 8. Pulse sequences for the DPFGSE experiment showing details of the timing scheme used. Sequence (a) is that recommended for routine measurements; it incorporates one nonselective 180° pulse, S_{null}, in the mixing time in order to improve suppression, see text for details. The delay d is included after each gradient to allow the spectrometer and field-frequency lock to recover from the effects of the gradient. An identical delay is included prior to each gradient partly for reasons of symmetry (see text for discussion) and partly to allow time for any circuit used to inhibit the field-frequency lock used during the gradient to be engaged. Any power switching needed can also be carried out during the delays d. The basic phase cycle is $\phi_1 = x, y, -x, -y$; $\phi_2 = x$, $\psi_1 = x, -x, x, -x$. This can be extended to 16 steps by adding EXORCYCLE to the second selective 180° pulse. Typically, all gradients are of duration 1 ms. Experience indicates that the a good choice for the ratio of G_1:G_2 is 7:3, and that the gradients $G_{m,1}$ and $G_{m,2}$ should by somewhat weaker than those used in the DPFGSE sequence; with these values, a maximum gradient strength of around 10 G cm^{-1} is sufficient. The value of d depends on the spectrometer hardware, but is typically 50–100 μs. The mixing time is $\tau_1 + \tau_2$, and typically $\tau_2 = 0.44\ \tau_m$. As described in the text, anti-phase contributions can be suppressed by using a selective 180° pulse at the end of the mixing time. Sequence (b), which replaces everything to the right of point B in sequence (a), shows the timing for this version of the experiment. The phase cycling is as before, and the frequency switching of $S_{m,1}$ is (4 × on-resonance, 4 × off-resonance). $G_{m,3}$ and $G_{m,4}$ are typically as $G_{m,1}$ and $G_{m,2}$. For more complete suppression of anti-phase contributions, two selective 180° pulses are needed. This is implemented in sequence (c) which replaces everything to the right of point B in sequence (a). The frequency switching is now $S_{m,2}$ = (4 × on-resonance, 4 × off-resonance), $S_{m,3}$ = (8 × on-resonance, 8 × off-resonance). The delay D is needed for both frequency switching and stabilization after a gradient; depending on the spectrometer hardware this may be different from the delay d. Frequency switching needed prior to $S_{m,1}$ or $S_{m,2}$ can take place during τ_m.

16, which itself is eight times longer than a conventional 180° pulse. The pulse has a ''WURST'' (*21*) amplitude profile $[1 - \sin(\pi t/t_p)^{20}]$, $-\frac{1}{2}t_p < t < \frac{1}{2}t_p$, and a nonlinear frequency sweep which has been numerically optimized to cover the desired bandwidth and range of radiofrequency field strengths, and which gives superior performance to a linear frequency sweep as originally proposed (*21*).

As was commented on above, it is important to ensure that the length and strength of the individual gradients are chosen so as to avoid refocusing of unwanted pathways, of which there are many if the pulses are imperfect. Some typical values for the gradients are suggested in the legend to Fig. 8. However, it should be emphasized that these are simply starting points and that some optimization will be needed for each particular experimental arrangement.

Ideally, a series of NOE spectra with increasing mixing times should be recorded as the development of the NOE enhancements can then be followed. If, however, time only permits recording a single spectrum, the issue arises of the choice of mixing time. For small to medium-sized molecules, a mixing time on the order of 0.5 s will generally give an NOE spectrum in which only short-range interactions give detectable enhancements. As these interactions are likely to be the most easily and unambiguously interpreted, such a spectrum is likely to be particularly useful in the initial stages of a structural study.

At longer mixing times, e.g., comparable with the longitudinal relaxation time, NOE enhancements resulting from long-range interactions may be seen. In addition, enhancements resulting from magnetization being transferred in two or more cross-relaxation steps may be seen. These kind of indirect transfers come about when magnetization from the target spin is first transferred to one spin, and then the same magnetization is further transferred to a third spin. As a result, the third spin shows an NOE enhancement even though it is not cross-relaxing with the target spin.

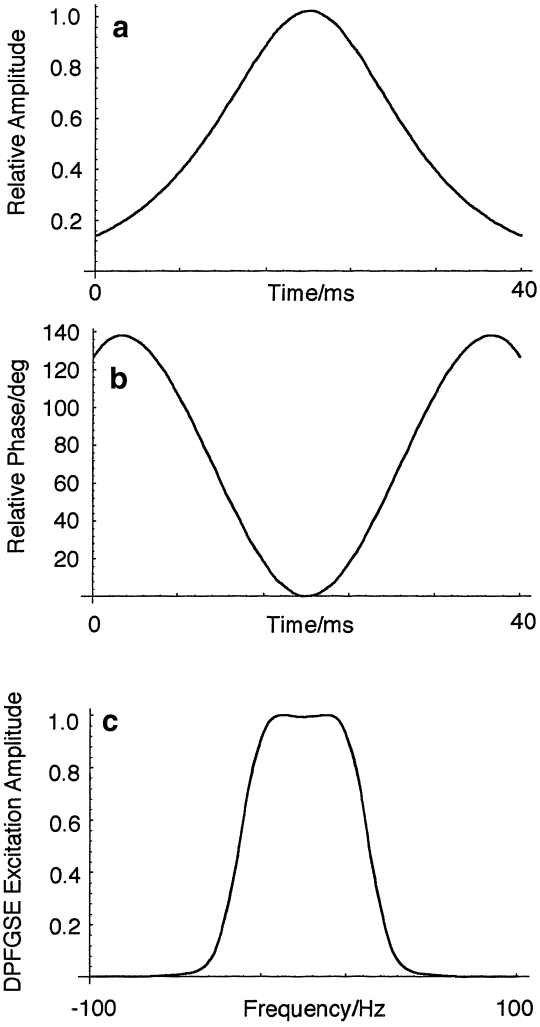

FIG. 9. Details of the frequency-modulated *selective* inversion pulse ''son2,'' described in the text. Plots (a) and (b) show the amplitude and phase profiles of a pulse of duration 40 ms. Plot (c) shows the calculated excitation profile that results when two son2 pulses are used in a DPFGSE sequence.

In the positive NOE region, these relayed enhancements show a characteristic pattern of signs: a spin receiving magnetization as a result of an odd number of sequential steps, e.g., one or three steps, experiences a positive enhancement while those spins receiving magnetization by an even number of steps, e.g., two, show negative enhancements. Of course, it is possible for a spin to receive magnetization by both a direct route and an indirect route. This can lead to the NOE enhancement changing sign as the mixing time is altered. For example, at short mixing times, the direct pathway may lead to a positive enhancement, but as the mixing time increases, an indirect pathway leading to a negative NOE enhancement may start to become significant. As a result, the enhancement begins to reduce and may eventually cross through zero and become negative. In such cases, a study of the NOE spectrum as a function of mixing time helps to reveal the cross-relaxation pathways that are taking place.

Quantification of Enhancements

It is common to quote the size of steady-state NOE enhancements as part of the process of reporting the data

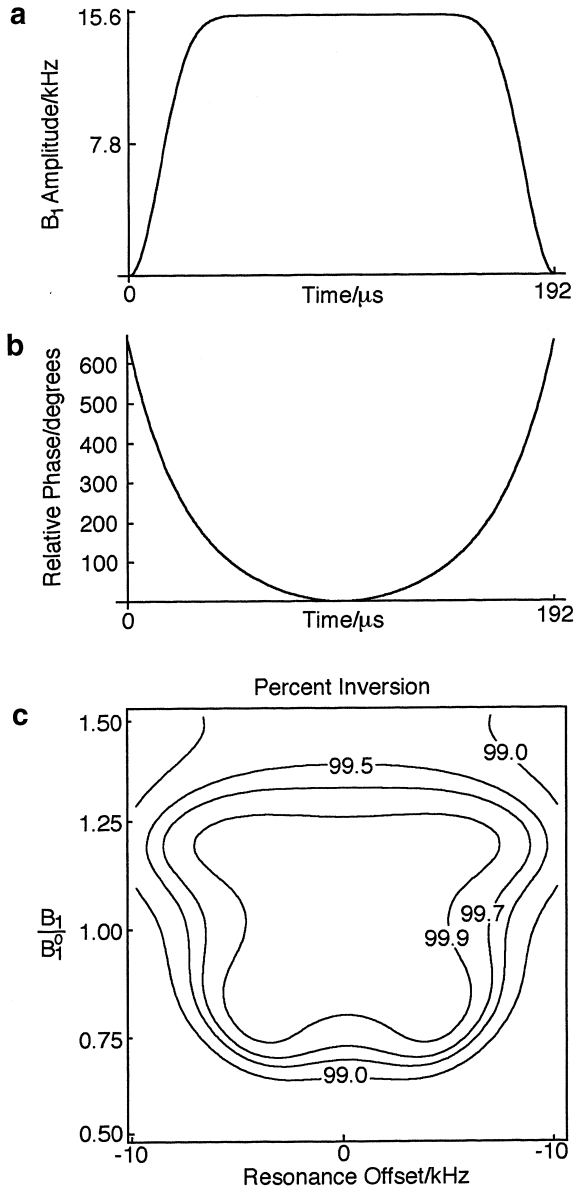

FIG. 10. Details of a frequency-modulated broadband inversion pulse suitable for use as a nulling pulse, S_{null}, during the mixing time of the DPFGSE NOE experiment. Plots (a) and (b) show the amplitude and phase profiles of a pulse of duration 192 μs. The contour plot (c) shows the calculated degree of inversion (expressed as a percentage) achieved by this pulse as a function of resonance offset and deviation of the radiofrequency field strength, B_1, from its nominal value, B_1°. The pulse has been designed to give excellent inversion over the whole proton chemical-shift range and to be tolerant of B_1 inhomogeneity.

on which a structure determination is based. Through experience the idea of what is a ''large'' or ''small'' NOE enhancement in a particular molecular system has grown up and in addition there is some notion of the limit below which an enhancement would generally be regarded as ''unreliable.''

The transient NOE experiments described in this paper on the whole give smaller NOE enhancements than are normally observed in steady-state experiments. There is thus a problem with quoting the numerical values of these transient enhancements as they will be out of line with the established scale for steady-state enhancements and may appear at first sight to be too small to be reliable. There is an additional problem in the case of the transient experiments that the enhancement depends on the choice of mixing time. In reporting the results of NOE experiments, it will therefore be essential to make it clear what kind of NOE experiment was used so that the reader uses an appropriate scale of what is a reasonable and reliable enhancement.

Distance Measurements

It is well known that relative internuclear distances can be estimated by exploiting the fact that the cross-relaxation rate constant between two spins is proportional to the inverse sixth power of the distance between them. This rate constant can be measured from the initial, linear part of the buildup curve of the NOE enhancement. Such a buildup curve is traditionally rather difficult to measure as in the linear region the NOE enhancements tend to be small and thus most easily perturbed by the presence of subtraction artifacts. It is a very attractive feature of the gradient-based experiments that the NOE spectra are of such high quality that it becomes much easier to measure these buildup curves.

For the case of the DPFGSE NOE experiment, it was shown above that the initial slope of the buildup curve of the fractional enhancement is $(1 + \alpha_1)\sigma_{12}$ (Eq. [29]). Therefore in order to be able to determine the cross-relaxation rate constant, we need to know the degree of inversion of the target spin, α_1. Probably the simplest way to measure this is to compare the integral of the target multiplet in a simple pulse-acquire spectrum, I_{ref}, with the integral in the DPFGSE NOE spectrum recorded using zero mixing time, I_0. It follows that $\alpha_1 = -(I_0/I_{\text{ref}})$, where the minus sign accounts for the usual phasing of the NOE spectrum which makes the target, and hence I_0, negative. Due to the gradients and other pulses that are contained within the mixing time it is not possible to record a spectrum with truly zero mixing time. However, a mixing time of a few milliseconds is usually sufficiently short that it can be taken as zero.

If the method described above is used to suppress antiphase contributions, the target multiplet is also suppressed in the NOE spectrum. It is then not possible to measure the integral of the target multiplet at zero mixing time from the experiment. Rather, a separate experiment in which the selective 180° pulse is either always present or always absent must be used. An alternative is to keep the spectra recorded with the selective 180° pulses on- and off-resonance separate so that α_1 can be estimated prior to adding the spectra together.

Once cross-relaxation rate constants have been measured, distances can be determined in one of two ways. The first is to use the value of the rate constant between two spins which are a known distance apart in order to establish the constant of proportionality between the inverse sixth power of the distance and the rate constant. The second is to make a separate determination of the correlation time, for example, from ^{13}C relaxation time and heteronuclear NOE measurements, and use this in conjunction with the well-known expression for the cross-relaxation rate constant (*2*) to convert the cross-relaxation rate constants to distances. Both of these approaches assume that all internuclear vectors in a molecule are undergoing the same isotropic motion characterized by a single correlation time.

RESULTS

Figure 11 shows a series of NOE spectra of 11β-hydroxyprogesterone, **2,** recorded using the DPFGSE NOE sequence. These spectra are very representative of the kinds of results that it is possible to achieve routinely in a relatively short time and on a few milligrams of a medium molecular weight compound. We have found that once a suitable set of parameters have been determined, even relatively inexperienced operators of the spectrometer can obtain excellent results, indicating that the experiment is tolerant and robust. The NOE spectra show the excellent selectivity that can be achieved with the DPFGSE sequence and are also free of visible subtraction artifacts. Typical NOE enhancements in these spectra are somewhat less than those measured in steady-state experiments, but the quality of the spectra is such that the smaller enhancements can be relied upon.

Figure 12 shows an NOE spectrum of 6(5H)-phenanthridinone, **1,** in which H_5 is the target and which was recorded using a mixing time of 8 s. This spectrum shows the direct positive enhancements of H_4 and H_6 and an indirect *negative* enhancement of H_9. Also visible is a *positive* enhancement of H_{10} which arises from a three step transfer $H_5 \rightarrow H_6 \rightarrow H_9 \rightarrow H_{10}$. That these enhancements do indeed arise from these pathways has been confirmed by measuring NOE spectra as a function of mixing time. The buildup curves shown in Fig. 13 are consistent with the expected dynamics for these relayed effects; the enhancement of H_{10} has a maximum of just 0.2%. We believe that this is the first time that such a three-step transfer has been detected in a molecule in the positive NOE region.

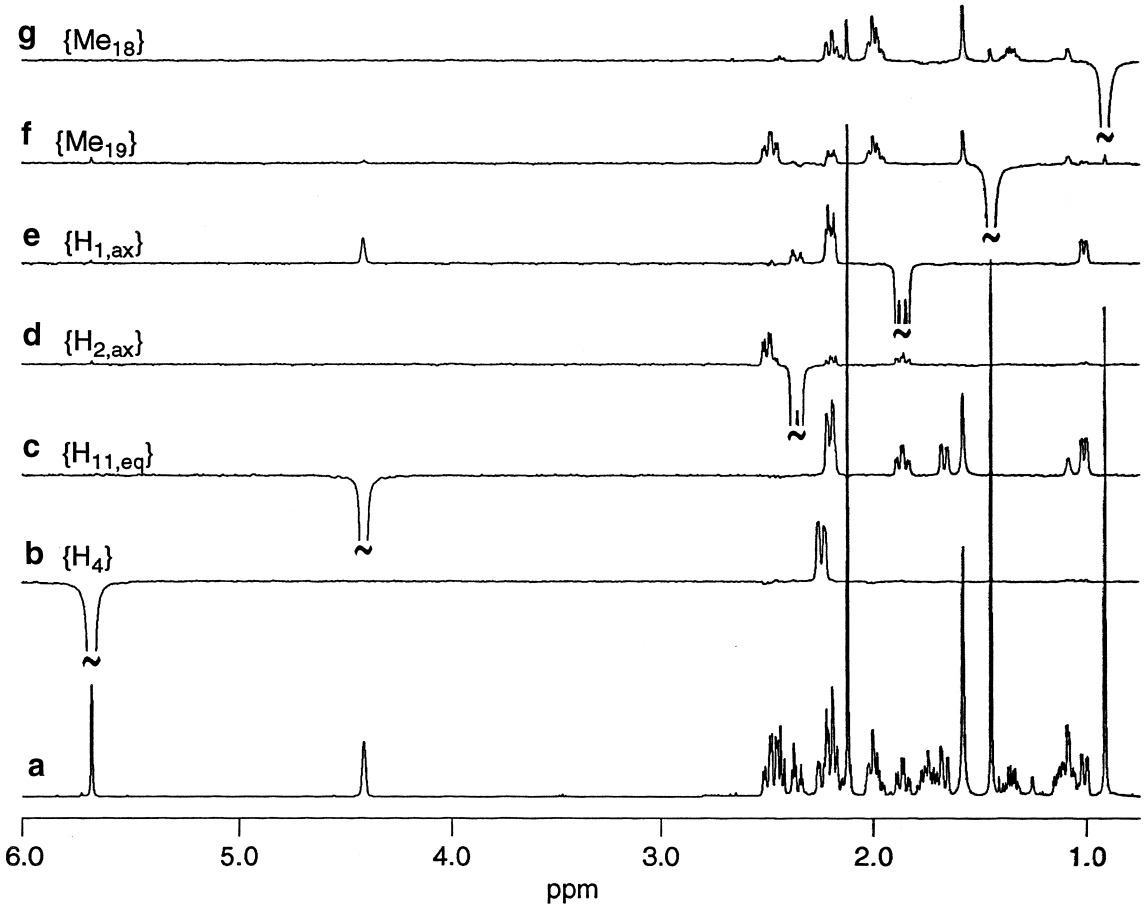

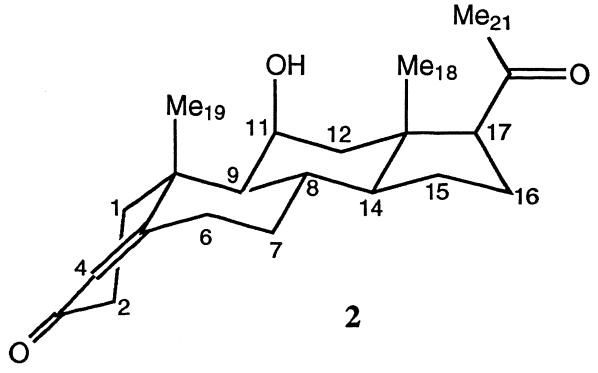

2

FIG. 11. NOE spectra of 11β-hydroxyprogesterone, **2,** recorded using the DPFGSE NOE sequence under typical conditions. The conventional spectrum is shown at the bottom and the remainder (b–g) are all NOE spectra with targets indicated in the usual way. In spectrum (g), the singlet (due to H_8) appearing at about 1.5 ppm shows an enhancement of around 8%. Each NOE spectrum was recorded in 90 minutes, and the sample concentration was 20 m*M* in $CDCl_3$. The mixing time, τ_m, was 2 s, and two nonselective inversion pulses were placed during this time at 0.33 and 0.83 τ_m. The selective pulses used in the DPFGSE sequence were all Gaussians truncated at the 1% level and of duration 7.5 ms for recording spectrum (c), 120 ms for recording spectrum (f), and 60 ms for the remainder.

We have also detected a negative NOE enhancement which is consistent with the *four-step* transfer to H_{11} (data not shown). The observation of these very small relayed effects is a testament to the extraordinary quality of the NOE spectra obtainable using the DPFGSE NOE experiment.

CONCLUSIONS

We have shown that the use of gradients in one-dimensional NOE experiments results in a substantial improvement in the quality of NOE spectra, thus making both qualitative and quantitative measurements easier and more reliable. It

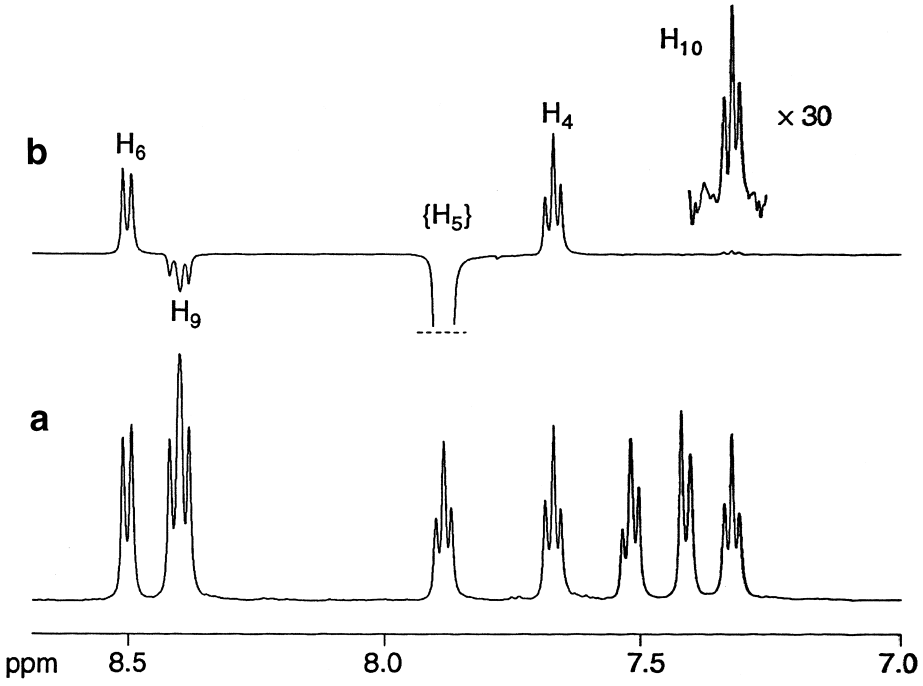

FIG. 12. The conventional (a) and NOE spectrum (b) of 6(5H)-phenanthridinone, **1,** illustrating the appearance of indirect NOE enhancements. With H_5 as the target, direct positive NOE enhancements are seen on H_6 and H_4. In addition, a relayed negative enhancement is seen on H_9 and a doubly relayed positive enhancement is seen on H_{10} (scale expansion inset). The experimental conditions are similar to those used to record the spectra in Fig. 11, and the mixing time was 8 s. The sample was made up in CD_3OD and degassed by the freeze–pump–thaw method.

has also been shown that the anti-phase contributions which are frequently troublesome in all types of NOE experiments can be suppressed by a simple modification of the basic DPFGSE NOE experiment. The indications are that the experiments described in this paper are robust and reliable, pointing to the eventual replacement of the conventional steady-state NOE experiment by these new techniques.

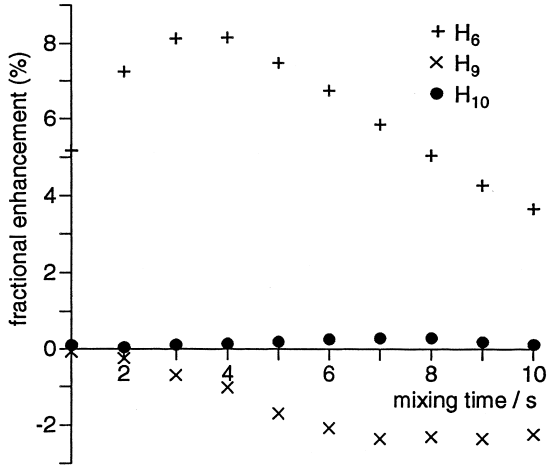

FIG. 13. NOE enhancement buildup curves for 6(5H)-phenanthridinone with H_5 as the target. The enhancements on H_6, H_9, and H_{10} show the characteristic sign and time dependence expected for direct, relayed, and doubly relayed NOE enhancements.

ACKNOWLEDGMENTS

This material is based on work partially supported by the National Science Foundation, CHE-9625674. Que Van acknowledges support from a Synthesis and Structure of Biological Macromolecules Training Grant (PHS GM 07311). We are grateful to Dr. David Neuhaus (MRC LMB, Cambridge) for helpful discussions, for his continuing interest in this project, and for a generous allocation of spectrometer time. We thank Charles Lyons for his helpful contributions. K.S. thanks the EPSRC for a CASE studentship, and the Shell Research Centre, Thornton, for generous support. The 500 MHz spectrometer used for part of this work was purchased with the aid of a grant from the EPSRC.

REFERENCES

1. J. H. Noggle and R. E. Schirmer, ''The Nuclear Overhauser Effect,'' Academic Press, New York, 1971.
2. D. Neuhaus and M. P. Williamson, ''The Nuclear Overhauser Effect in Structural and Conformational Analysis,'' Verlag Chemie, New York, 1989.
3. J. K. M. Sanders and J. D. Mersh, *Prog. NMR Spectrosc.* **15,** 353–400 (1982).
4. J. K. M. Sanders and B. K. Hunter, ''Modern NMR Spectroscopy,'' 2nd ed., Oxford Univ. Press, Oxford, 1993.
5. J. Jeener, B. H. Meier, P. Bachmann, and R. R. Ernst, *J. Chem. Phys.* **71,** 4546–4553 (1979).

6. J. Stonehouse, P. Adell, J. Keeler, and A. J. Shaka, *J. Am. Chem. Soc.* **116,** 6037–6038 (1994).
7. K. Stott, J. Stonehouse, T. L. Hwang, J. Keeler, and A. J. Shaka, *J. Am. Chem. Soc.* **117,** 4199–4200 (1995).
8. H. Kessler, H. Oschkinat, C. Griesinger, and W. Bermel, *J. Magn. Reson.* **70,** 106–133 (1986).
9. A. A. Bothner-By, R. L. Stephens, J-M. Lee, C. D. Warren, and R. W. Jeanloz, *J. Am. Chem. Soc.* **106,** 811–813 (1984).
10. L. Braunschweiler and R. R. Ernst, *J. Magn. Reson.* **53,** 521–528 (1983).
11. T. L. Hwang and A. J. Shaka, *J. Magn. Reson. A* **112,** 275–279 (1995).
12. C. Emetarom, T. L. Hwang, G. Mackin, and A. J. Shaka, *J. Magn. Reson. A* **115,** 137–140 (1995).
13. G. Bodenhausen, R. Freeman, and D. L. Turner, *J. Magn. Reson.* **27,** 511–514 (1977).
14. E. O. Stejskal and J. E. Tanner, *J. Chem. Phys.* **42,** 288–292 (1965).
15. R. A. Hoffman and S. Forsén, *Prog. NMR Spectrosc.* **1,** 15–204 (1966).
16. J. Keeler, D. Neuhaus, and M. P. Williamson, *J. Magn. Reson.* **73,** 45–68 (1987).
17. J. Baum, R. Tycko, and A. Pines, *Phys. Rev. A* **32,** 3435–3447 (1985).
18. M. S. Silver, R. I. Joseph, and D. I. Hoult, *Phys. Rev. A* **31,** 2753–2755 (1985).
19. R. Freeman, S. P. Kempsell, and M. H. Levitt, *J. Magn. Reson.* **38,** 453–479 (1980).
20. A. J. Shaka and R. Freeman, *J. Magn. Reson.* **55,** 487–493 (1983).
21. Ē. Kupče and R. Freeman, *J. Magn. Reson. A* **115,** 273–276 (1995).